Received: 13 September 2022 | Revised: 20 October 2022 | Accepted: 6 November 2022

DOI: 10.1002/aocs.12665

ORIGINAL ARTICLE

AOCS WILEY

Fast chromatography of pulse triacylglycerols

William Craig Byrdwell[1] | **Hari Kiran Kotapati**[1,2] | **Robert Goldschmidt**[1]

[1]Methods and Application of Food Composition Lab, Agricultural Research Service, U.S. Department of Agriculture, Beltsville, Maryland, USA

[2]Department of Nutrition and Food Science, College of Agriculture and Natural Resources, University of Maryland, College Park, Maryland, USA

Correspondence
William Craig Byrdwell, Methods and Application of Food Composition Lab, Agricultural Research Service, U.S. Department of Agriculture, Beltsville, MD 20705, USA.
Email: Craig.Byrdwell@usda.gov

Funding information
USDA Agricultural Research Service

Abstract

A short 10-min ultra high performance liquid chromatography (UHPLC) method was used for separation and lipidomic analysis of triacylglycerols (TAGs) in 10 pulses: baby lima beans, black beans, black-eyed peas, butter beans, cranberry beans, garbanzo beans, green split peas, lentils, navy beans, and pinto beans. The lipids extracted using chloroform/methanol averaged 1.9–2.7% across all pulses except garbanzo beans, which gave 6.2% lipids. TAGs were analyzed using dual parallel mass spectrometry (LC1MS2), areas were integrated using LipidSearch 4.2 software, and percent relative TAG compositions were calculated. Fatty acid response factors were calculated by comparison to calibrated GC-FID, which were used to calculate response-factor adjusted TAG compositions. Principal component analysis revealed that the pulses separated into three clusters, which were further highlighted using hierarchical cluster analysis. A subset of TAGs was quantified using calibration curves made from alternating sets of regioisomers in the non-linear high concentration range (~2.5 nMol/ml to ~300 nMol/ml). A linear calibration curve for the sum of tocopherols detected by fluorescence was constructed with a coefficient of determination, r^2, >0.99 for low concentrations (0.50–50 μg/ml), but tocopherols in pulses appeared to be inefficiently extracted. TAG regioisomers were quantified based on a Critical Ratio (CR), $[AA]^+/[AB]^+$, interpolated between the CRs of two pure regioisomer standards taken from alternating calibration standards. TAG mole percent relative compositions are reported for the first time for most pulses and the compositions are given with more detail and specificity than previously reported.

KEYWORDS
APPI-MS, beans, ESI-MS, legumes, mass spectrometry, triglycerides

INTRODUCTION

Legumes are plants that bear fruit in pods, and according to the Food and Agriculture Organization (FAO) of the United Nations (UN) (United Nations Food and Agriculture Organization, 2022), pulses are "dry seeds of leguminous plants which are distinguished from leguminous oil seeds by their low fat content." Furthermore, the UN FAO limits the definition to "…crops harvested solely for dry grain, thereby excluding crops harvested green for food which are classified as vegetable crops, as well as those crops used mainly for oil extraction and leguminous crops that are used exclusively for sowing purposes."

Oilseeds, most of which yield edible oils, such as soybeans (~20% fat, Pryde, 1980) and low erucic acid rapeseed (canola) oil (Dupont et al., 1989), etc. have been well studied, and fatty acid (FA) determinations (Dubois et al., 2007; Fedeli & Jacini, 1971) and triacylglycerol (TAG) composition analyses (Buchgraber et al., 2004; Zeitoun et al., 1991) have been reported for decades, using each new generation of chromatographic techniques (Dugo et al., 2008) and detectors, leading to the current era of mass spectrometry (Cao et al., 2017; Xu et al., 2018, 2020). Pulses by definition are low in fat, and are appreciated for their high fiber and high protein (Ferreira et al., 2021; Hall et al., 2017). Thus, their FA and TAG compositions have been investigated substantially less than those of oilseeds. The overall amount of fat is typically determined for pulses, but the detailed compositional analyses of pulse lipids are not as commonly reported as for oilseeds.

Despite the paucity of data on pulse oils, pulses are consumed in large quantities in the United States, at 11.7 lbs./person/year (U.S. Department of Agriculture, 2017). For this reason, we began investigating the detailed lipid compositions of market class pulses that are widely eaten by American consumers (Mitchell et al., 2021). We chose a subset of 10 commonly consumed pulses out of the 23 samples that colleagues previously analyzed to determine the amounts of mono-, di-, and oligosaccharides (Kotha et al., 2020), so we could build a more thorough picture of the complete nutritional profile of those pulses, and show correlations, if present, between oligosaccharides and lipids.

We have taken a two-pronged approach for analysis of pulse extract samples. First, a fast, high throughput method was applied that is intended to be an improvement over simple infusion, but which does not provide as much detailed information as more lengthy analyses. Second, a longer, multi-dimensional LC method that is more thorough and definitive has been applied. The results presented here are pursuant to the first goal, to provide high-throughput analyses that are better than simple infusion.

For these experiments we employed a dual parallel mass spectrometry (LC1MS2) approach similar to that we first reported (Byrdwell, 1998), though in this case we employed electrospray ionization (ESI) on a high-resolution accurate-mass (HRAM) orbitrap™ mass spectrometer in parallel with atmospheric pressure photoionization (APPI) on a tandem sector quadrupole (TSQ) instrument. Lipidomics was performed using LipidSearch software applied to the ESI-HRAM-MS data, while classical quantification using extracted ion chromatograms (EICs) was used for TAG quantification by APPI-MS, and fluorescence detection (FLD) was employed for quantification of extracted tocopherols.

EXPERIMENTAL PROCEDURES

Fatty acyl chain abbreviations

Fatty acyl chains on TAGs are named as fatty acids, in the form of CN:U, or carbon number (CN), the total number of carbon atoms in the fatty acyl chains, and the number of sites of unsaturation (U). In order of CN:U, the FA abbreviations are: 2:0, acetic acid, Ac; 4:0, butyric acid, Bu; 6:0, caproic, Co; 7:0, enanthic, En; 8:0, caprylic, Cy; 9:0, pelargonic, Pg; 10:0, capric, Ca; 11:0, undecanoic, Un; 12:0, lauric, La; 13:0, tridecanoic, Tr; 14:0, myristic, M; 15:0, pentadecanoic, Pn; 16:0, palmitic, P; 16:1, palmitoleic, Po; 17:0, margaric, Ma; 18:0, stearic, S; 18:1, oleic, O; 18:2, linoleic, L; 18:3, linolenic, Ln; 18:4, stearidonic, Sd; 19:0, nonadecanoic, No; 20:0, arachidic, A; 20:1, gadoleic, G; 21:0, heneicosanoic, He; 22:0, behenic, B; 22:1, erucic, E; 23:0, tricosanoic, Tc; 24:0, lignoceric, Lg; 24:1, nervonic, N; 26:0, cerotic, Ce.

Chemicals and samples

Solvents for LC were Optima™ grade from Fisher Scientific or spectrophotometric grade from Sigma Aldrich. Samples were ground from raw pulses and stored at −80°C. Market class pulses were obtained as ground samples from Prof. John Finley from Louisiana State University, via Dr. Dave Luthria and Dr. Raghavendhar Kotha, who previously analyzed these samples and reported the oligosaccharide contents (Kotha et al., 2020). Pulses were extracted using the method of Folch et al. (1957) with minor modifications (Byrdwell et al., 2022). Vitamin D2 was added prior to extraction, as an extraction internal standard (EIS) for fat-soluble vitamins (FSVs), and menaquinone, vitamin K2, was added prior to making sample to final volume in solution, as an analytical internal standard (AIS) for FSVs, both at a concentrations of 2.0 μg/ml. A sequence of runs consisted of seven calibration standards, a blank, 10 pulse samples, and a blank, repeated four times, plus a final set of calibration standards plus an extra final blank, such that there were five sets of seven standards, four sets of 10 pulse samples, and 10 blanks, for 85 runs. Fat-soluble vitamin (FSV) standard levels run were 0.05, 0.10, 0.25, 0.5, 1.00, 2.50, 5.00 μg/ml, as given in Table S1.

The mixture of TAGs used for quantification was intended primarily for milk and infant formula analysis, based on our previous report (Byrdwell et al., 2022), but we added polyunsaturated TAGs for pulse analysis (containing O and L, but not Ln, for stability). Four odd-chain fatty acid (FA) containing TAGs were used as EISs, tri-9:0, tri-13:0, tri-17:0, tri-21:0, and four odd-chain FA-containing TAGs were used as AISs, tri-7:0, tri-11:0, tri-15:0, tri-19:0. These latter were added in equimolar amounts (0.02062 μmol/ml) to directly demonstrate the different molar ionization efficiencies based on increasing carbon chain length.

Two sets of calibration standards were made, one from 1,3-TAG regioisomers and one from 1,2-TAG regioisomers, then a single set of calibration standards was made by combining alternating regioisomer standards from the two sets. Additionally, four Type III TAGs were included to confirm previous trends in Critical Ratio 2 (Byrdwell, 2005a, 2015a, 2016), which is $[AC]^+/([AB]^+ + [BC]^+)$ for Type III TAGs and $[AA]^+/[AB]^+$ for Type II TAGs. Standards 1, 3, 5, and 7 were from 1,3-TAG regioisomers; standards 2, 4, and 6 were from 1,2-TAG regioisomers. From these two sets of regioisomers the fragment ratios in mass spectra were used to construct regioisomer calibration lines for Type II TAGs, according to the equations proposed previously (Byrdwell, 2005b), giving secondary regioisomer calibration lines within the primary quantitation calibration curves.

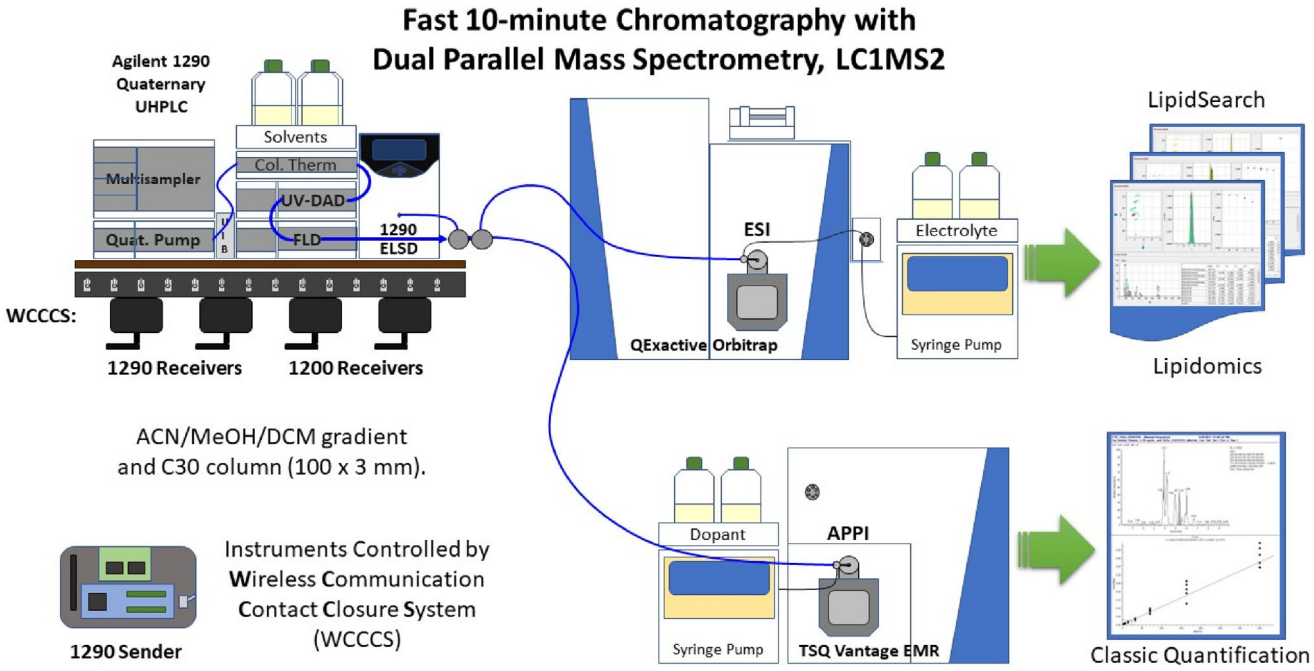

FIGURE 1 Diagram representing the arrangement of instruments in the dual parallel mass spectrometry (LC1MS2) experiments. TSQ, tandem sector quadrupole; EMR, extended mass range; ESI, electrospray ionization; APPI, atmospheric pressure photoionization; FLD, fluorescence detector; UV-DAD, ultraviolet diode array detector; ELSD, evaporative light scattering detector; ACN, acetonitrile; MeOH, methanol; DCM, dichloromethane

TAG regioisomer standards were so expensive we could only order the exact minimum amount available from Larodan Fine Chemicals (Monroe, MI), and these had to be quantitatively transferred to a volumetric flask. The 14 Type II TAG (Byrdwell, 2015a) regioisomer pairs that were used are: CaMCa/CaCaM, LaMLa/LaLaM, LaPLa/LaLaP, LaOLa/LaLaO, PLP/PPL, POP/PPO, LPL/LLP, OPO/OOP, LOL/LLO, OLO/OOL, OSO/OOS, SOS/SSO, OAO/OOA, ODhO/OODh. The four Type III TAG pairs were: POLa/OLaP, PLO/OPL, POS/SPO, SLO/SOL.

In addition to regioisomers, three mixtures of TAGs, and two pure TAGs (OOO and LLL) were added to quantify other TAG molecular species. Larodan TAG Mix 15 (#90-3015) contained equal weights of tri-C6:0, tri-8:0, tri-10:0, tri-12:0, tri-14:0, and tri-18:0. Sigma-Aldrich TAG Mix #17810 contained equal weights of tri-2:0, tri-4:0, tri-6:0, tri-8:0, and tri-10:0. Sigma-Aldrich TAG Mix #17811 contained equal weights of tri-8:0, tri-10:0, tri-12:0, tri-14:0, and tri-16:0. The combined concentrations of these mixtures and the specific concentrations of the regioisomers, which had different minimum purchase quantities, are given in Table S1.

Liquid chromatography

An Agilent 1290 Infinity Flex II ultra high performance liquid chromatography (UHPLC) system (Agilent Technologies, Inc., Santa Clara, CA) was used, which consisted of a G7167B multisampler, G7104A quaternary pump, G7116B thermostatted column compartment (TCC), G7117B diode array detector (DAD), G7121B fluorescence detector, and G1390B universal interface box (UIB) II to which was connected a G7167B evaporative light scattering detector (ELSD), as depicted in Figure 1. The column was a solid core, superficially porous 100.0 × 3.0 mm, 2.6 μm particle ThermoScientific Accucore C30 (part #27826-103030) maintained at 10°C in the TCC. Ten-microliter injections were used.

The ternary gradient with variable flow rate consisted of methanol (MeOH, solvent A), acetonitrile (ACN, solvent B), and dichloromethane (DCM, solvent D) is depicted in Figure S1. The gradient was as follows: 0 min: 0% A/80% B/20% D at 1.0 ml/min; 0.5 min: 0% A/80% B/20% D at 1.0 ml/min; 3.33 min: 43% A/31% B/26% D at 1.0 ml/min; 5.33 min: 2% A/60% B/38% D at 1.0 ml/min; 6.93 min: 1.8% A/40.2% B/58% D at 1.2 ml/min; 8.25 min: 0% A/10% B/90% D at 1.5 ml/min; 8.75 min: 0% A/10% B/90% D at 1.5 ml/min; 8.90 min: 0% A/80% B/20% D at 1.0 ml/min; 10.0 min: 0% A/80% B/20% D at 1.0 ml/min.

The detector settings were as follows: (1) DAD—210.0 nm (generic), 5.0 nm bandwidth (bw), 360.0 nm reference (ref); 248.0 nm (for tocopherols), 9.0 nm bw, 360.0 nm ref; 265.0 nm (for vitamin D), 9.0 bw, 360.0 nm ref; 297.0 nm (for vitamin K), 11.0 nm bw, 450.0 nm ref; 326.0 nm (for retinol), 11.0 nm bw, 450.0 nm ref; spectra from 190.0 to 400.0 nm, 2.0 nm

steps, slit 2.0 nm. (2) FLD—294 nm excitation wavelength (exc), 330 nm emission wavelength (em); multi-emission exc, 470 nm em. (3) ELSD—80°C evaporator, 90°C nebulizer, 1.30 gas, photomultiplier 1.0, acquired at 20 Hz by UIB II. Flow from the column went to a splitter comprised of two Valco tees (IDEX Health & Science, Oak Harbor, WA) in series. The bulk of effluent (~700 μl/min) went to the ELSD, with ~150 μl/min split to ESI-MS and ~150 μl/min to APPI-MS.

Mass spectrometry

ESI-MS and MS/MS data were acquired on a ThermoScientific QExactive high-resolution, accurate-mass (HRAM) mass spectrometer (Thermo Fisher Scientific, San Jose, CA) operated at its maximum resolution of 140,000. The sheath gas was at 25 arbitrary units (au), auxiliary and counter-current (sweep) gases at 0. The spray voltage was 4000 V and the probe heater was off. The scan range was *m/z* 150–1150, with the top four precursors selected for data-dependent acquisition (DDA) of MS/MS with an isolation window of 1.5 and normalized collision energy of 30. All data were acquired in centroid mode to minimize file sizes. The electronically actuated switch on the instrument was plumbed with deionized water and electrolyte solution made of 100 mM ammonium formate 1:4 in MeOH, for 20 mM NH_4OCOH. The switch was programmed to rinse the ESI probe with water between runs (from 9.95 min in each run to 0.05 min in the next run).

A ThermoScientific TSQ Vantage EMR unit-resolution tandem sector quadrupole (TSQ) mass spectrometer was used for atmospheric pressure photoionization (APPI). The sheath gas was 50 au, auxiliary gas was 10.0 au, and sweep gas at 3.0 au. The vaporizer temperature was 400°C and the capillary temperature was 250°C. Full scans were obtained throughout from *m/z* 150–1150 in 0.75 s with a peakwidth (pw) of 0.50 amu. Selected ion monitoring (SIM) and selected reaction monitoring (SRM) were conducted from 0 to 3.50 min. DDA of the top 2 precursor ions was conducted from 3.50 to 10.0 min.

SIM masses were as follows: *m/z* 269.227 (retinol), *m/z* 385.346 (vitamin D3, $[M + H]^+$), *m/z* 397.346 (vitamin D2, $[M + H]^+$), *m/z* 402.350 (δ-tocopherol $[M]^+\cdot$), *m/z* 416.365 (γ-tocopherol $[M]^+\cdot$), *m/z* 430.381 (α-tocopherol $[M]^+\cdot$), *m/z* 445.310 (menaquinone, vitamin K2, $[M + H]^+$), *m/z* 451.357 (phylloquinone, vitamin K1, $[M + H]^+$), *m/z* 473.399 (α-tocopherol acetate, $[M + H]^+$). MS/MS scan times were 0.15 s, with Q1 pw 0.70 and Q3 pw 0.50. Not all FSVs were observed in pulse samples. This method has been applied to a wide range of samples.

SRM transitions were as follows: *m/z* 269.227 → *m/z* 93.070 (retinol), *m/z* 385.346 → *m/z* 367.336 (vitamin D3), *m/z* 397.346 → *m/z* 379.336 (vitamin D2), *m/z* 402.350 → *m/z* 137.060 (δ-tocopherol $[M]^+$), *m/z* 416.365 → *m/z* 151.076 (γ-tocopherol $[M]^+$), *m/z* 430.381 → *m/z* 165.092 (α-tocopherol $[M]^+$), *m/z* 445.310 → *m/z* 187.076 (menaquinone, vitamin K2, $[M + H]^+$), *m/z* 451.357 → *m/z* 187.076 (phylloquinone, vitamin K1, $[M + H]^+$), *m/z* 473.399 → *m/z* 207.102 (α-tocopherol acetate, $[M + H]^+$). SRM scan times were 0.15 s, with Q1 pw 0.70 and Q3 pw 0.50.

Calculations, statistical analysis, and lipidomics

FSVs and TAGs in the calibration standards were quantified from both ESI-MS and APPI-MS data using the Quan Browser of Xcalibur (Thermo Fisher Scientific, San Jose, CA). Fluorescence detection of tocopherols was quantified using Chemstation C.01.09 (Agilent Technologies, Santa Clara, CA). Peak areas from all data systems were pasted into Microsoft Excel spreadsheets and quantified using the "linest()" function and response factors, due to the fact that we previously demonstrated that Agilent Chemstation results were not statistically valid due to point averaging (Byrdwell, 2019).

LipidSearch 4.2 was used for lipidomic analysis of TAGs, but we had to process files in a non-conventional way to overcome some inherent shortcomings in the software. The alignment process caused several problems. First, truncation of areas to four significant figures occurred when data were exported, resulting in loss of precision. Second, retention time (RT) variability caused truncation of peaks (splitting mid peak) if a narrow window (RT tolerance) was used, or caused merging of isomer peaks (if separated) if a wider RT window was used. To avoid these and other problems, each file was processed individually by setting both the control and the sample as the same file, so the averages equaled the original values with full numerical precision.

The LipidSearch parameters used were as follows: Search Type: Product, Experiment Type: LC, Precursor Tolerance: 5.0 ppm, Product Tolerance: 5.0 ppm, m-score threshold: 2.0, Toprank filter: On, Main node filter: All isomer peaks, m-Score Threshold: 5.0, c-Score Threshold: 2.0, FA Priority: On, ID Quality filter: A.

Areas from LipidSearch were pasted into Microsoft Excel and the TAG composition was calculated. Overlapped TAG isomers typically shared an overlapped diacylglycerol-like fragment, $[DAG]^+$, and these were apportioned using idealized fragment ratios for Type II TAGs, 2:1, and Type III TAGs, 1:1:1. Although this was not ideal, this approach produced the least uncertainty compared to other apportionment methods, and represents one of the compromises of fast analysis. Fortunately, most overlaps involved a minor TAG in the presence of a larger one, such that the apportionment

of a minor area in a $[DAG]^+$ fragment had minimal effect on the TAG composition. By using this approach, the differences between idealized and observed fragment ratios were small and limited to one of the multiple fragments used for each TAG, thereby minimizing the associated uncertainty. For ESI-MS data, the fragment abundances from MS/MS mass spectra of integrated areas in LipidSearch were captured and pasted into Excel for calculation of Critical Ratios (Byrdwell, 2015a). For APPI-MS, the beginning and ending integration window times from the Quan Browser report were pasted into the Xcalibur Qual Browser (Thermo Fisher Scientific, San Jose, CA) to obtain the mass spectral abundances and those were copied and pasted into Microsoft Excel for Critical Ratio (Byrdwell, 2015a) calculation. Regioisomer calibration lines were calculated in Microsoft Excel from Critical Ratio 2 for the Type II TAG regioisomers.

The method of Byrdwell et al. (1996, 2001) was used for calculation of response factors based on comparison to the calibrated GC-FID results. The weight percent GC-FID fatty acid composition was converted to a mole percent, and also the fatty acid (FA) composition from the raw TAG composition was calculated. Then, response factors were calculated for each FA. Next, FA RFs were multiplied together to get TAG RFs (Byrdwell et al., 2001). Then, the raw TAG percentage composition was multiplied by the TAG RFs and re-normalized to 100%, to produce the RF-normalized TAG composition. RFs that gave a zero value by either GC-FID or MS were given an RF = 1.0. The maximum value any RF was allowed to have was 4.0. This kept RFs of minor components from skewing accompanying FAs. For instance, 23:0 in navy beans was present at 0.02%–0.03% and gave a large RF, and 22:0 in green split peas gave a value of 0.00% (<0.005%) and gave a large RF, both of which were capped at 4.0. The 10 most abundant FAs used normally calculated RFs while 15 had RFs set to 1, all of which had percentages from 0.00% to 0.72% in all samples.

Principal component analysis (PCA) and hierarchical cluster analysis (HCA) were performed using Unscrambler X (formerly Camo Analytics, now AspenTech).

RESULTS AND DISCUSSION

Pulse sample masses and total extract masses are given in Supplementary Table 2. Pulses averaged 2.30 ± 0.29% lipids extracted from the average sample weight of 2.3260 ± 0.0920 g, except garbanzo beans (*Cicer arietinum*), which was 2.7 times higher at 6.18% extracted. These amounts are in good agreement with literature values for pulses (Mahadevappa & Raina, 1978; Meiners et al., 1976; Yoshida et al., 2005, 2007a, 2008), including garbanzo beans (chickpeas) (Mahadevappa & Raina, 1978; Serrano et al., 2017).

A portion of the extract was taken for GC-FID derivatization and analysis; specifically, an average of 17.63 ± 1.05% (9.22 ± 1.18 mg for most and 30.8 mg for garbanzo beans) was used for GC and the remainder used for LC–MS analysis. The average weight for LC–MS analysis was 43.86 ± 5.39 mg, except garbanzo beans, which gave an extract weight for LC–MS of 124.5 mg.

The sequence of analyses of 85 runs presented here averaged 11 min per run, with a 10 min programmed gradient and 1 min between runs, for a total run time of ~935 min, or ~15.6 h. Thus, these analyses were readily accomplished overnight, representing a high throughput alternative to infusion experiments, while providing more information.

Figures 2 and 3 depict the chromatographic separation of a black bean (*Phaseolus vulgaris*) lipid extract, by ESI-HRAM-MS and APPI-MS, respectively. ESI-MS was more sensitive and provided HRAM results, so those results are discussed in detail, whereas APPI-MS data were used mainly for confirmation and could not be processed using LipidSearch software, so are not discussed in detail. LipidSearch did not recognize diacylglycerol-like fragments, $[DAG]^+$, produced by APPI-MS (or APCI-MS), but instead treated every peak in a spectrum as a protonated molecule or designated adduct, leading to many false identifications.

TAGs were separated by partition number (PN), which is the carbon number, CN, minus two times the number of sites of unsaturation, U, or PN = CN − 2 × U. Note that the term equivalent carbon number (ECN) is often used interchangeably with partition number, but is actually distinct and more empirical (Podlaha & Töregård, 1982). Figure 2 shows peaks separated by PN, with several PNs having multiple isomers (e.g., LLL + LOLn, PN = 42) or other molecular species (e.g., LnPL) within the same PN, shown in Figure 2c. Of course, by infusion, these peaks would all be sent to the mass spectrometer simultaneously, requiring the theoretical $[M + NH_4 + 2 \times {}^{13}C]^+$ contribution from PN 40 be calculated and subtracted from the PN 42 $[M + NH_4]^+$ masses having the same CN but one less U. Chromatographically separating the PNs obviates the need for isotope correction. Some separation within PNs was possible, even using this short 10-min run, such as OOL, LLS, and SOLn in Figure 2c. But in general, many isomers were not fully resolved using this short, fast separation, as expected.

ESI-MS of TAGs

Figure 2d shows the elution of AISs, demonstrating that the peak shapes were good, despite the short run. The sizes of the peaks of the equimolar AISs decreased

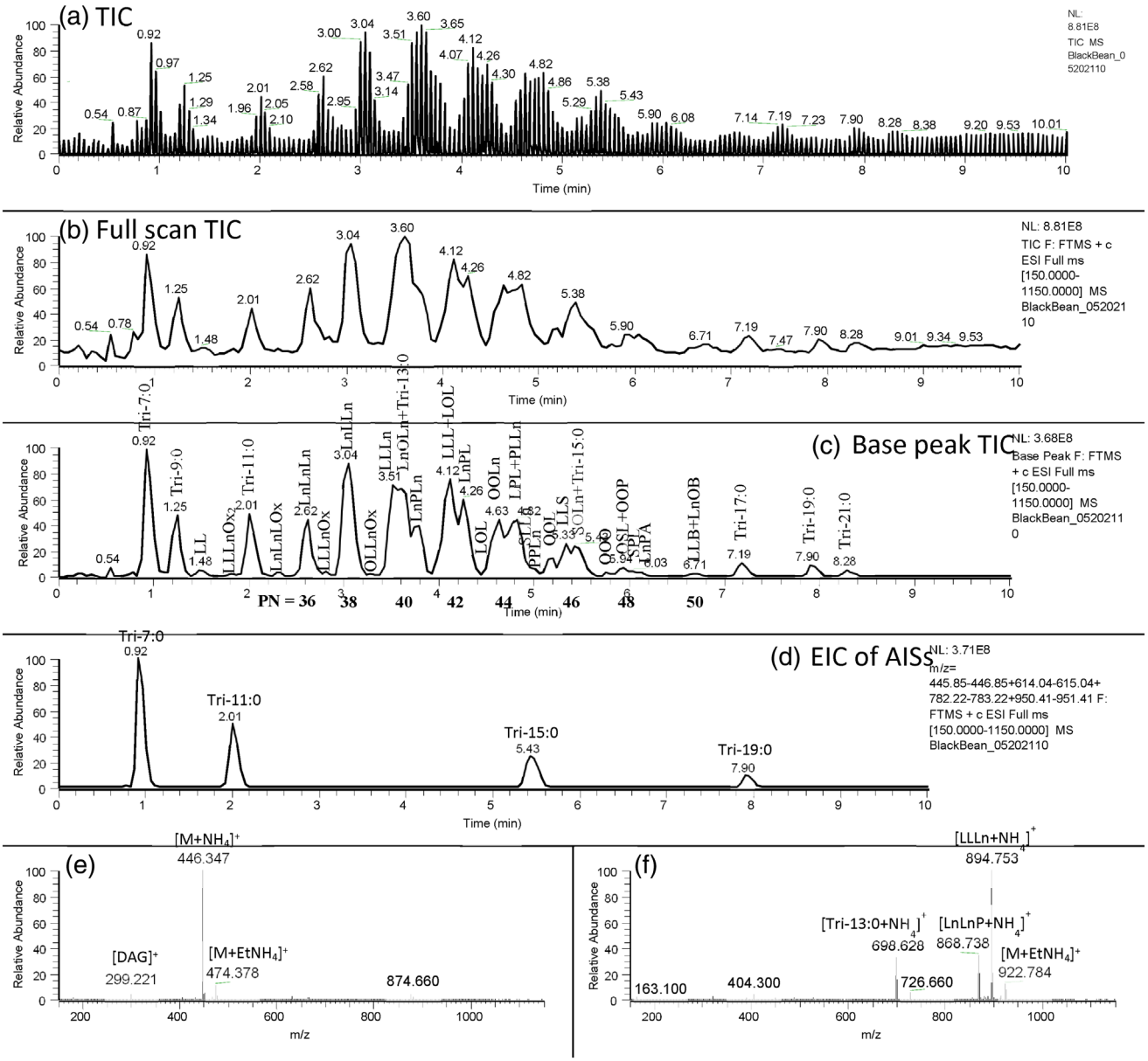

FIGURE 2 ESI-MS chromatograms and mass spectra of black bean extract. (a) Total ion current chromatogram (TIC); (b) full-scan TIC; (c) base peak chromatogram with partition numbers (PN = CN − 2xU) labeled; (d) extracted ion chromatogram (EIC) of analytical internal standards (AISs), tri-7:0, tri-11:0, tri-15:0, and tri-19:0; (e) average mass spectrum across tri-7:0 at 0.92 min; (f) average mass spectrum across peaks from 3.39–3.90 min, showing tri-13:0, LLLn + LnLnO, and LnLnP.

with increasing carbon chain length and retention time (RT) by ESI-MS, depicted in Figure S2, confirming previously reported trends (Duffin et al., 1991; Han & Gross, 2001). Because of its relatively high signal, 7:0/7:0/7:0 was used as the TAG analytical internal standard for further absolute quantification calculations.

The solvent gradient was designed to maximize the separation of early-eluting species, which are polyunsaturated TAGs in pulses, and short-chain saturated TAGs in milk and infant formula. The ternary gradient depicted in Supplementary Figure 1 shows the nonlinear nature of the gradient with low gradient slopes at early RTs. The larger RT gap between tri-11:0 (triundecanoin) at ∼2.0 min and tri-15:0 (tripentadecanoin) at ∼5.4 min in Figure 2d reflects this elution gradient.

Figure 2e,f shows that ESI-MS produced primarily intact ammonium adducts (e.g., EnEnEn $[M + NH_4]^+$ at *m/z* 446.347; LLLn $[M + NH_4]^+$ at *m/z* 894.753; LnLnP $[M + NH_4]^+$ at *m/z* 868.738), with only small amounts of diacylglycerol-like fragments, $[DAG]^+$, such as $[EnEn]^+$ at *m/z* 299.221 in Figure 2e, and these mostly from short-chain saturated TAGs. Short-chain TAGs also produced low levels of $[2\ M + NH_4]^+$, such as *m/z* 874.660 in Figure 2e (calculated mass: $2 \times 428.314 + 18.034 = 874.662$, $\Delta = 2.3$ ppm).

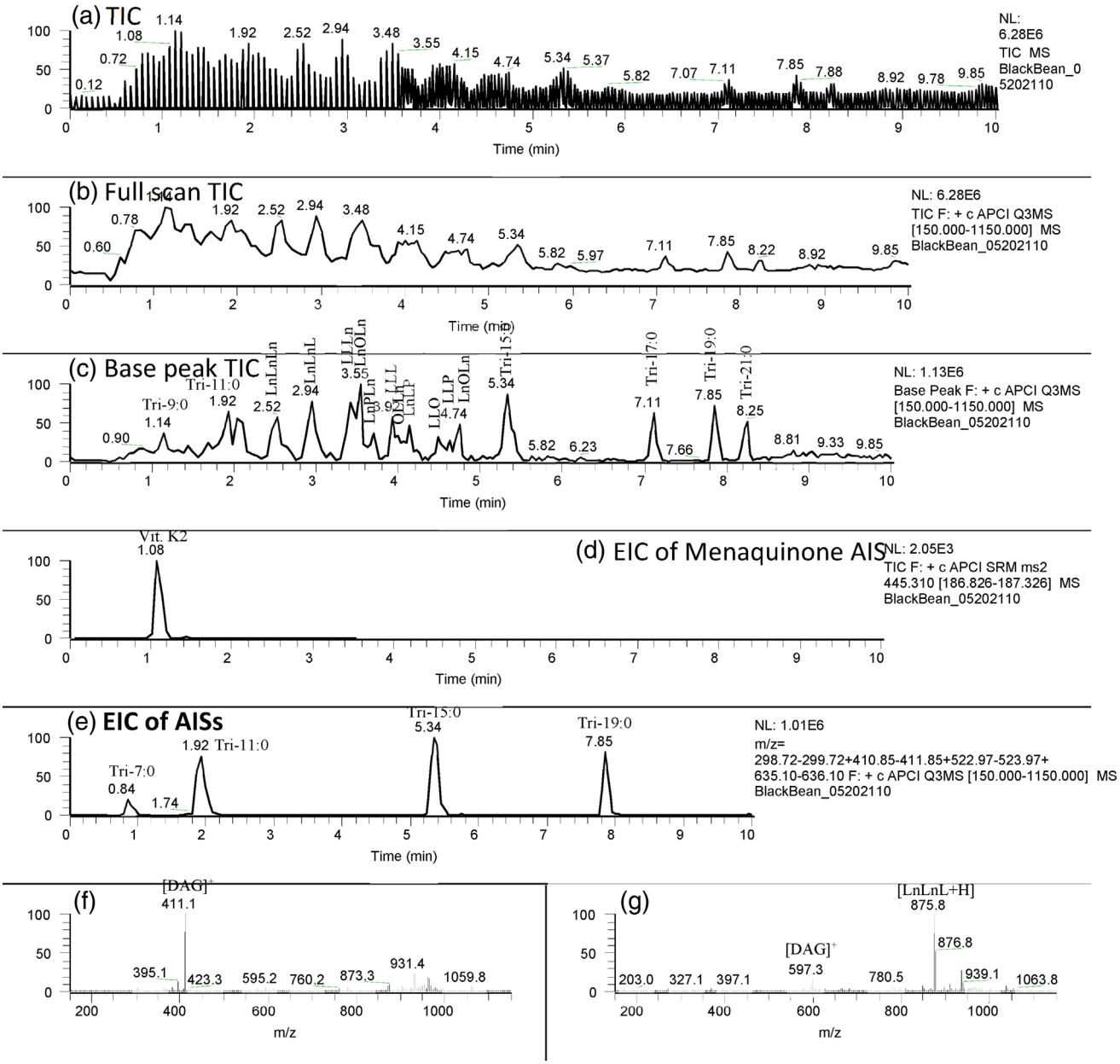

FIGURE 3 APPI-MS chromatograms and mass spectra of black bean extract. (a) Total ion current chromatogram (TIC); (b) full-scan TIC; (c) base peak chromatogram; (d) selected ion monitoring (SRM) chromatogram of analytical internal standard (AIS) menaquinone, or vitamin K2; (e) EIC of TAG AISs, tri-7:0, tri-11:0, tri-15:0, and tri-19:0; (f) average mass spectrum across tri-11:0 at 1.92 min; (g) average mass spectrum across peaks from 2.82–3.10 min, showing LnLnL

Since the solvent gradient included acetonitrile, CH_3CN, ethylamine, $CH_3CH_2NH_2$, was formed in the ESI source (Gu et al., 2006), and produced $[M + CH_3CH_2NH_3]^+$, or $[M + EtNH_3]^+ = [M + 46]^+$ adducts, such as *m/z* 474.378 in Figure 2e. Figures S3 and S4 show the ESI-MS chromatograms of the other nine pulse samples, with Figure S3 showing baby lima bean (*Phaseolus lunatus*), black-eyed pea (*Vigna unguiculata*), butter bean (*Phaseolus lunatus*) and cranberry bean (*Phaseolus vulgaris*) extract chromatograms and Figure S4 showing garbanzo bean (*Cicer arietinum*), green split pea (*Pisum sativum*), lentil (*Lens culinaris*), navy bean (*Phaseolus vulgaris*), and pinto bean (*Phaseolus vulgaris*) extract chromatograms.

TAG percent relative quantification

Table 1 provides the compositions of TAGs from the 10 pulse extracts as determined by LipidSearch analysis. Table 1 is sorted from top to bottom in order of average TAG compositions across all samples. The most abundant two TAGs were PLL and PLLn, averaging 10.67% and 10.45%, respectively, mostly because

TABLE 1 Triacylglycerol (TAG) percent relative compositions of pulses, arranged in decreasing order from top to bottom using average TAG composition across all samples

TAG[a]	RT[b]	Pinto bean	Navy bean	Cranberry bean	Black bean	Black-eyed peas	Lima bean	Butter bean	Lentils	Green Split peas	Garbanzo bean
PLL	4.737	5.13	6.38	5.83	4.59	12.07	19.57	21.18	12.09	11.09	8.79
PLLn	4.226	16.14	13.08	13.47	9.56	14.32	12.55	14.34	5.99	3.90	1.19
LLLn	3.479	9.58	10.21	9.24	6.41	8.92	6.77	5.29	5.20	4.78	2.46
OLL	4.584	1.93	4.13	3.05	4.25	1.03	3.64	1.79	12.32	13.37	17.83
POL	5.344	2.50	3.80	3.79	5.99	3.13	5.45	4.26	10.64	9.76	8.74
LLL	4.031	1.70	3.46	2.08	1.73	2.13	7.84	5.03	8.80	9.89	15.32
LLnLn	3.003	15.44	11.12	11.08	6.64	5.06	1.77	1.44	0.93	0.44	0.12
OLLn	4.031	6.26	7.79	8.25	8.49	1.88	1.73	1.11	5.13	4.70	1.80
PPL	5.535	2.56	2.09	2.06	1.95	8.50	9.58	12.09	3.21	2.39	2.01
PLnLn	3.715	11.85	7.39	8.43	5.60	5.12	2.45	2.78	0.63	0.14	0.03
POLn	4.745	5.35	5.38	6.91	9.26	2.53	1.93	2.36	2.99	2.20	0.62
OOL	5.191	0.44	1.75	1.13	3.34	0.00	0.42	0.19	8.47	9.77	14.06
PPLn	4.980	3.34	2.53	2.53	2.33	7.43	3.79	4.60	0.65	0.00	0.07
OOP	5.954	0.46	1.21	1.03	3.11	0.45	0.68	0.45	4.07	4.56	5.43
PSL	6.070	0.50	0.59	0.58	0.71	2.99	4.19	5.97	0.82	1.73	0.00
OLnLn	3.481	4.46	3.82	4.69	4.62	0.00	0.00	0.16	0.24	0.00	0.00
OOO	5.705	0.00	0.48	0.35	1.33	0.59	0.34	0.39	1.93	2.29	7.39
OOLn	4.585	1.21	1.84	2.17	5.30	0.10	0.00	0.06	1.92	1.14	0.31
SLLn	4.798	1.42	1.63	1.60	1.02	2.00	2.03	2.60	0.40	1.16	0.00
PPO	6.124	0.00	0.87	1.06	1.89	1.21	1.26	1.71	1.93	1.88	1.51
SLL	5.300	0.36	0.53	0.43	0.43	1.87	2.73	2.77	0.76	2.12	0.88
SOL	5.911	0.27	0.39	0.45	0.87	0.50	1.07	0.79	1.86	4.69	1.39
LnLnLn	2.574	4.21	2.22	2.77	1.77	0.55	0.11	0.10	0.00	0.00	0.00
PSLn	5.608	0.00	0.63	0.57	0.58	1.72	1.13	1.62	0.00	0.00	0.00
SLnLn	4.334	0.96	0.91	0.91	0.75	0.59	0.42	0.48	0.00	0.00	0.00
LLnB	6.044	0.46	0.56	0.45	0.48	1.11	0.37	0.82	0.26	0.00	0.00
PLLg	7.468	0.00	0.26	0.42	0.36	0.92	0.59	0.96	0.30	0.23	0.05
LLnLg	6.717	0.66	0.45	0.59	0.34	0.78	0.51	0.62	0.10	0.00	0.00
OOS	6.591	0.00	0.00	0.00	0.23	0.00	0.00	0.00	0.69	1.35	1.42
LLA	5.958	0.00	0.15	0.06	0.11	0.53	0.76	0.60	0.59	0.55	0.30
PLA	6.754	0.00	0.17	0.00	0.18	0.69	0.59	0.83	0.21	0.18	0.23
SOLn	5.312	0.38	0.53	0.62	0.68	0.00	0.24	0.22	0.12	0.26	0.00
PSO	6.777	0.00	0.00	0.00	0.31	0.32	0.38	0.43	0.00	0.84	0.67
LLLg	7.088	0.00	0.20	0.00	0.07	0.53	0.49	0.70	0.32	0.22	0.12
LLB	6.636	0.00	0.20	0.09	0.13	1.01	0.38	0.00	0.37	0.00	0.27
OLG	5.723	0.00	0.00	0.00	0.00	0.00	0.00	0.00	0.45	0.34	0.44
OLLg	7.384	0.00	0.27	0.00	0.39	0.35	0.26	0.00	0.32	0.24	0.17
OLA	6.586	0.00	0.00	0.00	0.19	0.15	0.00	0.00	0.48	0.50	0.66
PoLnLn	3.031	0.68	0.00	0.61	0.45	0.00	0.00	0.00	0.00	0.00	0.00
LLG	5.130	0.00	0.00	0.00	0.00	0.00	0.00	0.00	0.49	0.30	0.33
OOG	6.271	0.00	0.00	0.00	0.19	0.35	0.00	0.16	0.17	0.09	0.35
PPoL	4.743	0.00	0.00	0.00	0.00	0.00	0.00	0.00	0.71	0.60	0.30
LnLnLg	6.174	0.57	0.33	0.44	0.00	0.28	0.00	0.00	0.00	0.00	0.00
MLL	4.119	0.00	0.00	0.00	0.00	0.00	0.27	0.00	0.68	0.40	0.26
PLB	7.138	0.00	0.00	0.00	0.00	0.77	0.27	0.00	0.00	0.08	0.05

(Continues)

TABLE 1 (Continued)

TAG[a]	RT[b]	Pinto bean	Navy bean	Cranberry bean	Black bean	Black-eyed peas	Lima bean	Butter bean	Lentils	Green Split peas	Garbanzo bean
LnLnA	4.960	0.60	0.25	0.25	0.19	0.17	0.09	0.00	0.00	0.00	0.00
LnLnB	5.589	0.37	0.29	0.30	0.26	0.31	0.00	0.00	0.00	0.00	0.00
LLnG	4.624	0.21	0.34	0.27	0.13	0.23	0.00	0.00	0.24	0.00	0.00
PLnB	6.854	0.00	0.20	0.00	0.28	0.92	0.00	0.00	0.00	0.00	0.00
SSL	6.754	0.00	0.03	0.00	0.03	0.19	0.33	0.37	0.06	0.28	0.09
OLB	7.076	0.00	0.00	0.12	0.29	0.19	0.00	0.00	0.42	0.00	0.30
OLnA	5.968	0.00	0.29	0.29	0.40	0.10	0.00	0.15	0.00	0.00	0.02
LLEd	4.360	0.00	0.00	0.53	0.00	0.68	0.00	0.00	0.00	0.00	0.00
PLnA	6.195	0.00	0.19	0.00	0.16	0.39	0.14	0.26	0.00	0.00	0.00
OLnB	6.645	0.00	0.19	0.22	0.48	0.13	0.04	0.00	0.09	0.00	0.00
PLnLg	7.271	0.00	0.20	0.00	0.22	0.40	0.12	0.00	0.00	0.00	0.00
PnLL	4.437	0.00	0.00	0.00	0.00	0.00	0.76	0.00	0.00	0.00	0.16
MOL	4.743	0.00	0.00	0.00	0.00	0.00	0.00	0.00	0.47	0.30	0.12
PnOL	5.055	0.00	0.00	0.00	0.00	0.00	0.00	0.00	0.00	0.74	0.12
PLG	5.923	0.00	0.00	0.00	0.00	0.32	0.00	0.00	0.25	0.00	0.00
LLTc	6.869	0.00	0.00	0.00	0.00	0.33	0.00	0.00	0.37	0.00	0.09
MPL	4.894	0.00	0.00	0.00	0.00	0.00	0.24	0.00	0.36	0.00	0.10
LLnTc	6.397	0.00	0.24	0.00	0.00	0.21	0.00	0.00	0.00	0.00	0.00
OLnLg	7.099	0.00	0.16	0.00	0.31	0.07	0.04	0.00	0.00	0.00	0.00
PPP	6.401	0.00	0.00	0.00	0.00	0.40	0.17	0.00	0.00	0.00	0.00
PMaL	5.824	0.00	0.00	0.00	0.00	0.29	0.28	0.00	0.00	0.00	0.00
LLnA	5.468	0.00	0.00	0.24	0.00	0.32	0.00	0.00	0.00	0.00	0.00
OOA	7.076	0.00	0.00	0.00	0.00	0.00	0.00	0.00	0.00	0.19	0.31
OOLg	7.595	0.00	0.00	0.00	0.00	0.37	0.00	0.00	0.00	0.06	0.07
MaLLn	4.544	0.00	0.18	0.00	0.14	0.00	0.17	0.00	0.00	0.00	0.00
PnLLn	3.957	0.00	0.00	0.00	0.00	0.00	0.46	0.00	0.00	0.00	0.00
LLMa	4.974	0.00	0.00	0.00	0.00	0.00	0.28	0.00	0.00	0.00	0.18
SSLn	6.195	0.00	0.04	0.00	0.04	0.12	0.09	0.15	0.00	0.00	0.00
POB	7.486	0.00	0.00	0.00	0.22	0.11	0.00	0.00	0.00	0.00	0.11
PoLL	4.018	0.00	0.00	0.00	0.00	0.00	0.00	0.00	0.00	0.00	0.40
PLCe	7.687	0.00	0.00	0.00	0.00	0.19	0.00	0.00	0.00	0.18	0.00
PLTc	7.344	0.00	0.00	0.00	0.00	0.35	0.00	0.00	0.00	0.00	0.00
PoOL	4.713	0.00	0.00	0.00	0.00	0.00	0.00	0.00	0.00	0.00	0.34
POG	6.586	0.00	0.00	0.00	0.00	0.00	0.00	0.00	0.05	0.00	0.15
OOB	7.456	0.00	0.01	0.00	0.06	0.00	0.00	0.00	0.02	0.00	0.20
MaOL	5.631	0.00	0.00	0.00	0.00	0.00	0.00	0.00	0.00	0.00	0.28
OLnG	5.148	0.00	0.00	0.00	0.00	0.00	0.00	0.00	0.08	0.06	0.00
OLE	6.269	0.00	0.00	0.00	0.00	0.00	0.00	0.00	0.24	0.00	0.00
SLB	7.461	0.00	0.01	0.00	0.03	0.15	0.00	0.00	0.02	0.00	0.01
SLLg	7.668	0.00	0.00	0.00	0.00	0.06	0.00	0.15	0.00	0.00	0.01
OL17:1	4.904	0.00	0.00	0.00	0.00	0.00	0.00	0.00	0.00	0.00	0.23
LL17:1	4.294	0.00	0.00	0.00	0.00	0.00	0.00	0.00	0.00	0.00	0.21
PMaLn	5.319	0.00	0.00	0.00	0.00	0.18	0.00	0.00	0.00	0.00	0.00
PLnCe	7.507	0.00	0.00	0.00	0.00	0.13	0.00	0.00	0.00	0.00	0.00
MLLn	3.643	0.00	0.00	0.00	0.00	0.00	0.13	0.00	0.00	0.00	0.00
LnLnG	6.170	0.00	0.00	0.00	0.10	0.00	0.00	0.00	0.00	0.00	0.00

(Continues)

TABLE 1 (Continued)

TAG[a]	RT[b]	Pinto bean	Navy bean	Cranberry bean	Black bean	Black-eyed peas	Lima bean	Butter bean	Lentils	Green Split peas	Garbanzo bean
PO17:1	5.666	0.00	0.00	0.00	0.00	0.00	0.00	0.00	0.00	0.00	0.11
OOMa	6.242	0.00	0.00	0.00	0.00	0.00	0.00	0.00	0.00	0.00	0.10
OL17:2	4.294	0.00	0.00	0.00	0.00	0.00	0.00	0.00	0.00	0.00	0.09
OLHn	6.852	0.00	0.00	0.00	0.00	0.00	0.00	0.00	0.00	0.00	0.09
POA	7.204	0.00	0.00	0.00	0.00	0.00	0.00	0.00	0.00	0.00	0.09
OLnTc	6.862	0.00	0.00	0.00	0.00	0.00	0.00	0.00	0.08	0.00	0.00
OLTc	7.255	0.00	0.00	0.00	0.00	0.00	0.00	0.00	0.00	0.00	0.08
LLHn	6.229	0.00	0.00	0.00	0.00	0.00	0.00	0.00	0.00	0.00	0.08
PL17:1	5.044	0.00	0.00	0.00	0.00	0.00	0.00	0.00	0.00	0.00	0.07
SLnLg	7.507	0.00	0.00	0.00	0.00	0.07	0.00	0.00	0.00	0.00	0.00
OOTc	7.523	0.00	0.00	0.00	0.00	0.00	0.00	0.00	0.00	0.00	0.06
SLA	7.139	0.00	0.00	0.00	0.00	0.00	0.03	0.00	0.00	0.00	0.02
SLnB	7.274	0.00	0.00	0.00	0.00	0.05	0.00	0.00	0.00	0.00	0.00
SLnA	6.858	0.00	0.01	0.00	0.00	0.04	0.00	0.00	0.00	0.00	0.00
OLn17:1	4.552	0.00	0.00	0.00	0.04	0.00	0.00	0.00	0.00	0.00	0.00
OO17:2	4.904	0.00	0.00	0.00	0.00	0.00	0.00	0.00	0.00	0.00	0.04
POLg	7.706	0.00	0.00	0.00	0.00	0.00	0.00	0.00	0.00	0.00	0.03
SSO	7.204	0.00	0.00	0.00	0.00	0.00	0.00	0.00	0.00	0.00	0.03
LGB	7.309	0.00	0.00	0.00	0.00	0.02	0.00	0.00	0.00	0.00	0.00
SOG	7.079	0.00	0.00	0.00	0.00	0.00	0.00	0.00	0.00	0.02	0.00
PO17:2	5.044	0.00	0.00	0.00	0.00	0.00	0.00	0.00	0.00	0.00	0.01
SOB	7.706	0.00	0.00	0.00	0.00	0.00	0.00	0.00	0.00	0.00	0.01
SOA	7.489	0.00	0.00	0.00	0.00	0.01	0.00	0.00	0.00	0.00	0.00
LAB	7.698	0.00	0.00	0.00	0.00	0.00	0.00	0.00	0.00	0.00	0.00
LnAB	7.507	0.00	0.00	0.00	0.00	0.00	0.00	0.00	0.00	0.00	0.00
	Sum	100.00	100.00	100.00	100.00	100.00	100.00	100.00	100.00	100.00	100.00

Note: Columns arranged by decreasing percentage of LLnLn, indicated by principal component analysis. Averages of four replicates.
[a]Abbreviations in Materials and Methods.
[b]Average retention time across all pulse samples.

of their high levels in baby lima beans and butter beans (some sources refer to regular lima beans as butter beans, which are both *Phaseoulus lunatus*, while others indicate that they differ). Figure 4 provides a graphical representation of the top 30 average TAGs, arranged in order of decreasing LLnLn.

A plot of the PCA of the TAGs in Figure 4 is shown in Figure 5. PCA caused the TAGs to cluster into three groups, highlighted by ovals in Figure 5. Of course, baby lima beans and butter beans clustered together (middle in Figure 4), along with black-eyed peas, which share similar high levels of PLLn, LLLn, PPL, and PLL. Four pulses clustered together, pinto beans, navy beans, cranberry beans, and black beans, due to their similar low levels of PLL combined with high levels of LLnLn, OLLn, and PLnLn. A third cluster, made up of lentils, green split peas and garbanzo beans (chick-peas), shared similar levels of OLL, POL, LLL, and OOL. The loading plot from PCA, Figure S5, confirms that the molecular species above are responsible for most of the difference between samples. LLnLn, PLnLn, and OLLn are in the lower left quadrant of Figure S5 and correspond to cluster 1. PLLn, PPL, and PLL are in the left and upper parts of the graph, and correspond to cluster 2. OLL, OOL, LLL, and POL are in the lower right area of the graph, and correspond to cluster 3. The clusters identified by PCA were confirmed by HCA, depicted in Figure 6. Three clusters were selected based on the PCA results, and the samples fell into the same clusters by HCA as by PCA. The fact that sorting the TAG compositions by LLnLn caused them to cluster into the same groups in Figure 4 as found by PCA, and the association of other TAGs with specific clusters leads to the conclusion that some TAGs, such as LLnLn may be useful as biomarkers to differentiate *Phaseolus vulgaris* (common beans) from other types, such as lima beans (*Phaseoulus lunatus*), etc.

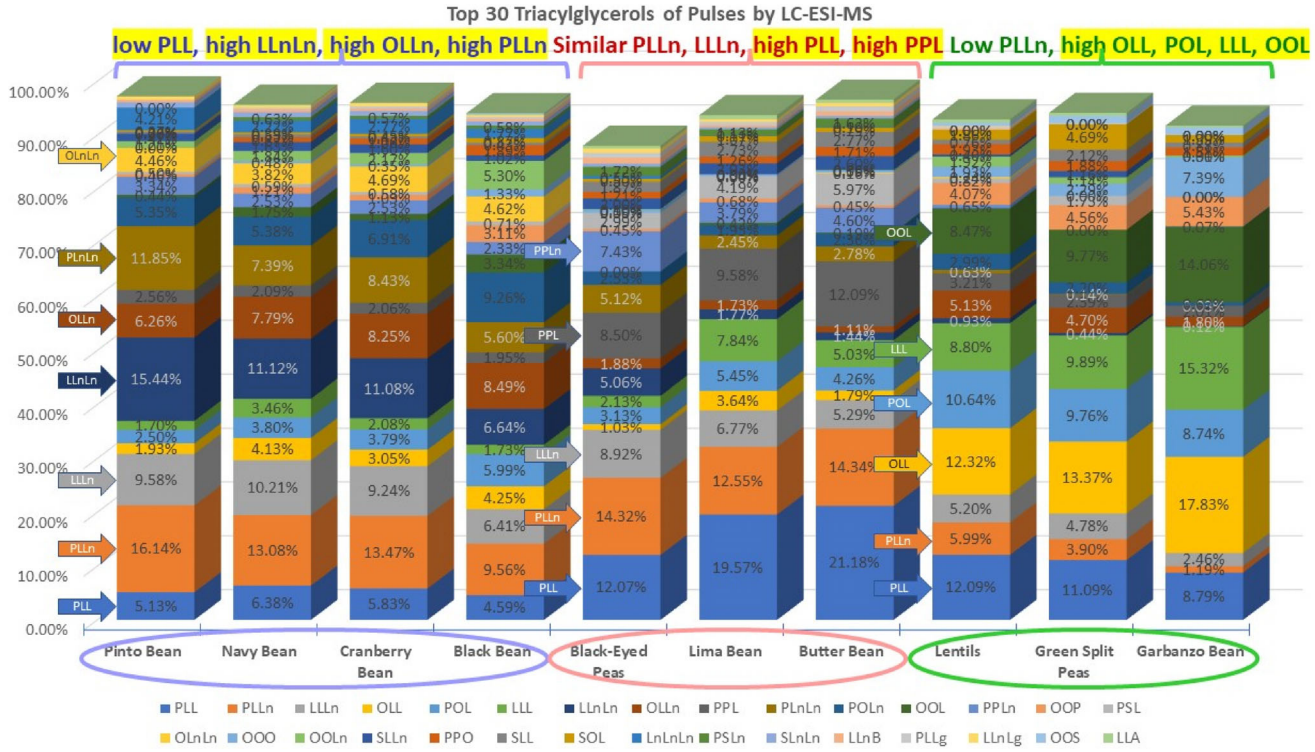

FIGURE 4 Stacked bar chart showing the composition of the top 30 most abundant triacylglycerol (TAG) molecular species, sorted from left to right by decreasing LLnLn (abbreviations in materials and methods). Sorting by this one TAG put the TAG compositions in the same order that they clustered into using principal component analysis (PCA), indicated by the highlighting ovals. See PCA of TAGs in Figure 5

FIGURE 5 Principal component analysis (PCA) of triacylglycerol molecular species. Ovals added to highlight clusters

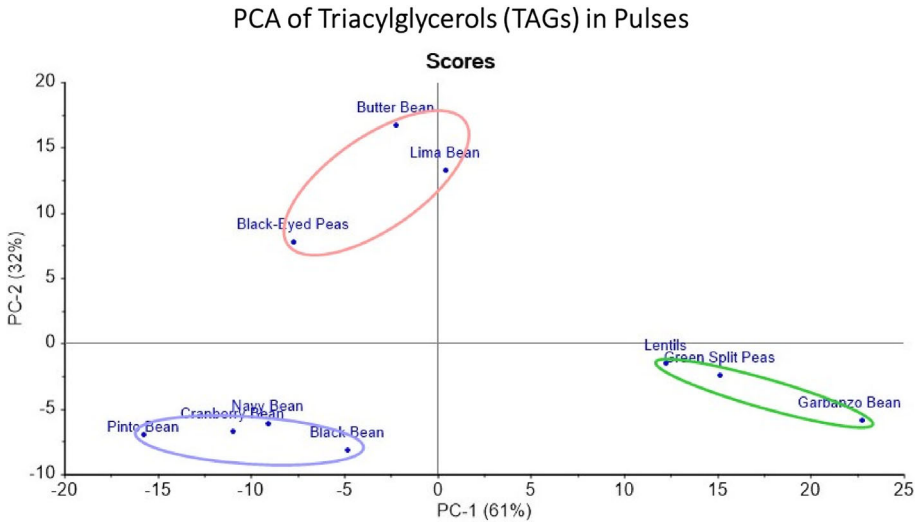

We chose to analyze these specific samples because they were part of the 23 pulses that had been previously analyzed for oligosaccharides (Kotha et al., 2020). HCA of the oligosaccharides (OSs) resulted in five clusters, but gave similar clustering for some pulse varieties. Specifically, black beans (*Phaseolus vulgaris*), navy beans (*Phaseolus vulgaris*), and pinto beans (*Phaseolus vulgaris*) clustered together based on OSs similar to how they clustered based on TAGs. Black-eyed peas (*Vigna unguiculata*) and baby lima beans (*Phaseolus lunatus*) clustered together based on both oligosaccharides and TAGs. Other pulses clustered differently. Cranberry beans (*Phaseolus vulgaris*) and green split peas (*Pisum sativum*) clustered together by OSs, but not TAGS. Lentils (*Lens culinaris*) and garbanzo beans (*Cicer arietinum*) were in separate clusters by OSs, but grouped together by TAGs, based on their higher compositions of OOL,

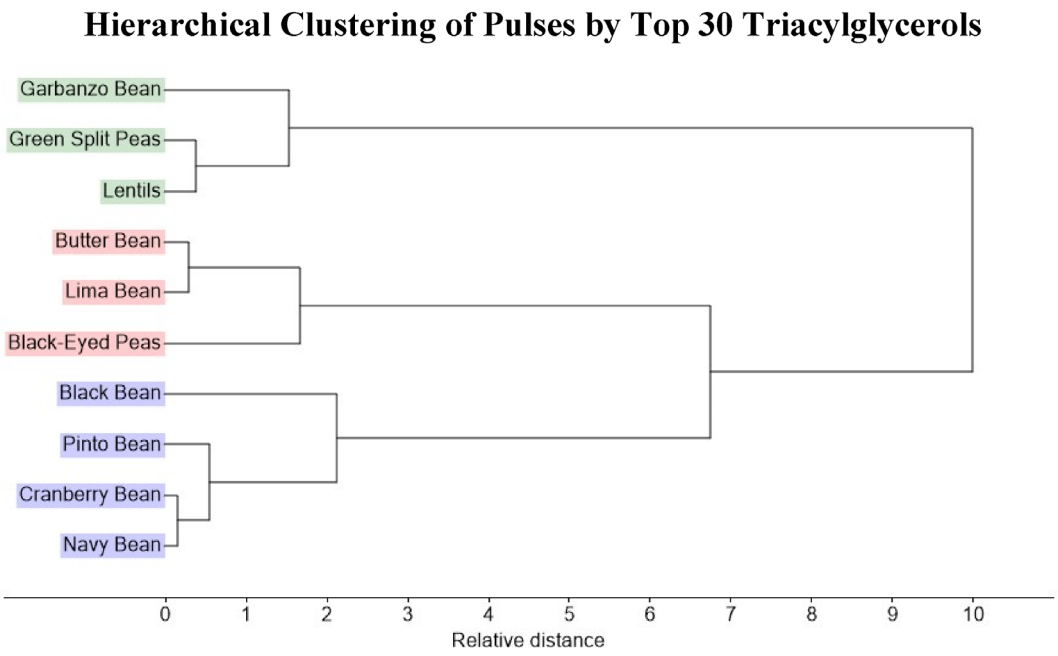

FIGURE 6 Hierarchical cluster analysis (HCA) using correlation of the molecular species compositions of triacylglycerols of pulses. Number of clusters set at 3 from principal component analysis.

LLL, POL, and OLL. Thus, there is some interesting agreement, but also some important differences between the groups classified by OSs (Kotha et al., 2020) and the clusters identified by TAGs. As we continue to analyze TAGs in additional pulse types, additional clusters may become apparent.

The HCA showed similarities to the clustering observed in the phylogeny of the pulses. According to Lavin et al. (2005), who examined the evolutionary rates of legumes, garbanzo beans (*Cicer arietinum*), green peas (*Pixum sativum*), and lentils (*Lens culinaris*), which grouped together in Figure 6, are all part of the "inverted-repeat-loss clade" (IRLC) crown node that evolved 39.0 $\pm$ 2.4 million years ago (MYA). Peas and lentils had a most recent common ancestor (MRCA) 17.5 $\pm$ 1.9 MYA and clustered quite closely by HCA in Figure 6. On the other hand, the *Phaseolus vulgaris* (black, cranberry, navy, and pinto beans) and *Vigna unguiculata* (black-eyed peas) are part of the millettioid crown node dating to 45.2 $\pm$ 1.7 MYA (along with *Glycine max*, soybeans). Black-eyed peas and common beans shared a MRCA 8.0 $\pm$ 0.8 MYA. Although black-eyed peas clustered with *Phaseolus lunatus* samples (baby lima beans and butter beans), they showed similarity to *Phaseolus vulgaris* in the amounts of several TAG molecular species (e.g., LLnLn, PLnLn, and others).

There are a few examples of TAG molecular species analyses of pulses, mostly by Yoshida and coworkers. Yoshida et al. (2008) used Ag-NO_3 thin layer chromatography (TLC) to physically collect and determine the molecular species composition of broad bean (*Vicia faba*), in mg/100 beans (not mol%). These were first separated by partition number (48–56), and then by FA degree of unsaturation for saturated (S), monounsaturated (M), di-unsaturated (D), and tri-unsaturated (T) FAs. Although this approach makes it a little more difficult to directly compare molecular species, the high levels of MD_2 and D_3 indicate high levels of OLL and LLL, and the SD_2 indicated substantial PLL. From the discussion of PCA above, the high MD_2 and D_3 with moderate SD_2 compared to Figure 4 indicates that the broad beans would likely cluster close to group 3, the lentils/green split peas/garbanzo bean group, than the groups that contained more DT_2 (LLnLn) and D_2T (LLLn).

Yoshida et al. (2005) took the same approach to TAG molecular species analysis of different cultivars of kidney beans (*Phaseolus vulgaris*), this time in mg/200 beans. There were substantially more T and D FAs in kidney beans than broad beans (above), with the substantial amount of T_3 (i.e., LnLnLn), DT_2 (LLnLn) as the major TAG, and high D_2T (LLLn), and substantial MDT (OLLn) all indicating that kidney beans are similar to Figure 4 group 1 TAGs, which is expected, since those are also *Phaseolus vulgaris*. MT_2 (OLnLn) appears higher in that report than reported here, but group 1 in Figure 4 did have the highest OLnLn. Thus, in terms of overall trends, our results agree well with other reports of pulse TAG compositions.

Omachi et al. (1987) performed analysis of winged bean (*Psophocarpus tetragonolobus*) TAGs by

collecting HPLC fractions and analyzing the FA compositions of each fraction. That bean was unique in its unusually high content of behenic acid (22:0). The most abundant TAG was reported to be OLB (21.3%), with OOB and OOO at 15.6% and 10.5%, respectively. The high proportion of "OL" and "OO" moieties indicates that winged beans are much more similar to Figure 4 group 3 pulses than other types having more polyunsaturated FAs.

Fatty acid compositions from TAGs

The fatty acid (FA) compositions given in Table 2 were calculated from the response-factor-normalized TAG percent relative compositions in Table 1 compared to the FA composition determined by calibrated GC-FID. The agreement between the calculated FA compositions and the empirical FA compositions was good, and appeared better than that produced by alternative quantification approaches, as discussed in our recent chapter (Byrdwell, 2020). FA isomers were not differentiated by LC–MS, so FAs are presented only by carbon number: degree of unsaturation (C:U). Isomers were identified by GC-FID retention time and mass spectra in GC–MS data. The complete composition of FAs including *cis*, *trans* and double bond location isomers is reported separately.

PCA of the FA compositions calculated from TAGs is given in Figure S6. In the PCA scores plot, the FAs clustered into the same three groups of pulse samples that were formed by PCA of the intact TAGs shown in Figure 5. The PCA loadings plot Figure S6B, showed that the FAs responsible for the majority of variance were the four most abundant FAs listed in Table 2 (16:0, 18:1, 18:2, and 18:3). The PCA of the FA compositions determined by GC-FID showed the same behavior and similar plots by PCA, reported separately.

TAG calibration curves

It was hypothesized that it might be possible to go from a percent relative composition to absolute quantification by quantifying one or more TAGs absolutely, and then using the percentage composition to scale all other TAGs relative to the one quantified absolutely. Unfortunately, this was not successful. While we were able to quantify some specific TAG molecular species, which amounts in mg are given in Table S2, the total weight of all TAGs, in milligrams, when scaled by the percentages (and converted from moles to mgs) in Table 1 did not add up to the measured extract mass. It appears that when the FA RFs were multiplied together to give TAG RFs and those were applied and the total was renormalized, the direct correlation between the peak area ratio to the internal standard and concentration in nMol/ml TAGs was lost.

In the past, we (Byrdwell et al., 1996) and other researchers have demonstrated linear calibration curves with high coefficients of determination (r^2) for TAGs at low levels. For this report, we characterized calibration curves for TAGs at higher levels. While we quantified FSVs in the range of μg/ml to ng/ml (below), we quantified TAGs in the range of mg/ml (e.g., for OOO, 884.8 g/mol, 0.1 mg/ml = 113 nMol/ml). In this concentration range, calibration curves were not best fit in Excel by linear equations, but by either polynomial functions, $y = a^*x^2 + b^*x + c$, or power functions, $y = a^*x^p$, where y is the peak area ratio to the internal standard (7:0/7:0/7:0) and x is the concentration in nMol/ml. Example calibration curves for PLP/PPL showing both polynomial and power functions to describe the nonlinear behavior of TAGs in the nMol/ml range are given in Figure 7. We also investigated other quantification approaches (response factors, point-to-point calibration, etc.), but they all gave results similar to those presented in Table S2.

Manual quantification of TAGs in the calibration mixture using Quan Browser in Xcalibur™ took advantage of the Byrdwell carbon isotope advantage reported in 2013 (Byrdwell, 2013), which included the first ^{13}C isotopic peak to increase signal by ~25%–65% with no loss of specificity. For example, the *m*/*z* 446.347 base peak of EnEnEn in Figure 2e has a $1 \times {}^{13}C$ peak at *m*/*z* 447.350 with an abundance of 27.10%, while NoNoNo (peak in Figure 2d, spectrum not shown) has an observed $[M + NH_4]^+$ base peak at *m*/*z* 950.910, with its observed $1 \times {}^{13}C$ isotope peak at *m*/*z* 951.913 with an abundance of 65.72%. Since TAGs are differentiated by at least one site of unsaturation, for 2 amu, the inclusion of $[M + NH_4 + 1]^+$ does not overlap with any other TAG mass, and provides essentially 'free' additional signal. Thus, the processing method for quantification included both $[M + NH_4]^+$ and $[M + NH_4 + 1]^+$ ions, giving maximum sensitivity without loss of specificity. TAG quantification using LipidSearch, on the other hand, used only monoisotopic masses.

Since application of RFs disrupted the direct relationship between peak areas and absolute amounts, absolute quantification of TAGs for which calibration curves were not constructed was not further pursued. Perhaps the most relevant shortcoming of this approach was that due to the expense of the regioisomer TAGs, we had to rely on the supplier for accurate weights, and that these had to be quantitatively transferred to the calibration stock solutions. Better results (e.g., higher r^2) would be expected if samples were affordable enough to purchase excess and weigh all samples in lab, as we did with less expensive components in the TAG mixture.

TABLE 2 Mole percentage fatty acid compositions calculated from response-factor-normalized triacylglycerols (TAGs) and from GC-FID (converted from weight %)

	Pinto bean		Cranberry bean		Navy bean		Black bean		Black eyed pea		Butter bean		Lima bean		Lentils		Green Split peas		Garbanzo bean	
FA	LC-MS	GC-FID	LC-MS	GC-FID	LC-MS	GC-FID	LC-MS	GC-FID	LC-MS	GC-FID	LC-MS	GC-FID	LC-MS	GC-FID	LC-MS	GC-FID	LC-MS	GC-FID	LC-MS	GC-FID
12:0[a]	0.00	0.00	0.00	0.00	0.00	0.00	0.00	0.00	0.00	0.00	0.00	0.00	0.00	0.00	0.00	0.03	0.00	0.00	0.00	0.01
14:0	0.00	0.10	0.00	0.07	0.00	0.06	0.00	0.12	0.00	0.15	0.00	0.44	0.21	0.20	0.50	0.52	0.23	0.25	0.16	0.15
15:0	0.00	0.21	0.00	0.13	0.00	0.12	0.00	0.22	0.00	0.08	0.00	0.55	0.41	0.42	0.00	0.19	0.25	0.24	0.09	0.09
16:0	17.91	20.59	17.45	19.12	16.83	17.70	17.83	18.99	27.93	28.62	30.75	33.26	26.79	27.95	16.90	17.37	14.67	15.17	11.32	11.35
16:1[b]	0.23	0.35	0.20	0.34	0.00	0.20	0.15	0.37	0.00	0.12	0.00	0.24	0.00	0.18	0.24	0.20	0.20	0.17	0.34	0.33
17:0	0.00	0.00	0.00	0.00	0.06	0.00	0.05	0.00	0.16	0.00	0.00	0.00	0.24	0.00	0.00	0.00	0.00	0.00	0.18	0.00
17:1	0.00	0.08	0.00	0.19	0.00	0.09	0.01	0.12	0.00	0.02	0.00	0.04	0.00	0.03	0.00	0.09	0.00	0.03	0.21	0.01
17:2	0.00	0.00	0.00	0.00	0.00	0.00	0.00	0.00	0.00	0.00	0.00	0.00	0.00	0.00	0.00	0.00	0.00	0.00	0.05	0.00
18:0	1.30	1.62	1.72	1.96	1.79	1.93	1.92	2.07	3.66	3.58	5.36	5.55	4.36	4.45	1.60	1.55	4.25	4.32	1.55	1.49
18:1[b]	8.46	8.60	13.06	12.96	12.89	12.69	22.37	21.53	5.35	5.24	5.30	5.33	6.42	6.22	24.79	24.08	27.03	26.18	34.32	34.43
18:2[b]	28.66	27.73	29.74	29.29	32.92	32.53	26.09	25.97	35.33	35.73	42.10	38.93	45.96	45.10	45.05	44.96	45.84	46.06	47.95	48.36
18:3[b]	42.49	38.85	36.39	33.92	33.85	32.61	29.73	28.27	22.95	21.96	14.74	13.37	14.03	13.49	8.95	8.61	6.45	6.20	2.26	2.24
19:0	0.00	0.03	0.00	0.03	0.00	0.02	0.00	0.03	0.00	0.02	0.00	0.04	0.00	0.02	0.00	0.04	0.00	0.04	0.00	0.01
20:0	0.20	0.31	0.28	0.37	0.35	0.36	0.41	0.43	0.80	0.77	0.61	0.57	0.54	0.50	0.43	0.45	0.48	0.47	0.54	0.52
20:1	0.07	0.10	0.09	0.12	0.11	0.14	0.14	0.15	0.31	0.29	0.05	0.10	0.00	0.11	0.58	0.60	0.27	0.28	0.42	0.40
20:2	0.00	0.03	0.18	0.03	0.00	0.03	0.00	0.02	0.23	0.09	0.00	0.03	0.00	0.03	0.00	0.08	0.00	0.05	0.00	0.05
20:3	0.00	0.02	0.00	0.02	0.00	0.02	0.00	0.02	0.00	0.05	0.00	0.00	0.00	0.00	0.00	0.02	0.00	0.00	0.00	0.00
21:0	0.00	0.00	0.00	0.00	0.00	0.00	0.00	0.00	0.00	0.00	0.00	0.00	0.00	0.00	0.00	0.00	0.00	0.00	0.06	0.00
22:0	0.28	0.42	0.40	0.51	0.49	0.55	0.74	0.82	1.60	1.60	0.27	0.40	0.36	0.36	0.40	0.45	0.03	0.12	0.32	0.30
22:1	0.00	0.00	0.00	0.01	0.00	0.00	0.00	0.00	0.00	0.02	0.00	0.00	0.00	0.00	0.08	0.10	0.00	0.01	0.00	0.01
23:0	0.00	0.25	0.00	0.19	0.08	0.18	0.00	0.24	0.29	0.24	0.00	0.24	0.00	0.16	0.15	0.18	0.00	0.06	0.08	0.07
24:0	0.41	0.61	0.48	0.58	0.62	0.66	0.56	0.54	1.28	1.26	0.81	0.79	0.67	0.67	0.35	0.36	0.25	0.24	0.15	0.14
24:1	0.00	0.00	0.00	0.00	0.00	0.00	0.00	0.00	0.00	0.00	0.00	0.00	0.00	0.00	0.00	0.03	0.00	0.00	0.00	0.00
25:0	0.00	0.07	0.00	0.10	0.00	0.07	0.00	0.05	0.00	0.07	0.00	0.08	0.00	0.06	0.00	0.07	0.00	0.04	0.00	0.01
26:0	0.00	0.04	0.00	0.08	0.00	0.05	0.00	0.03	0.11	0.09	0.00	0.04	0.00	0.04	0.00	0.03	0.06	0.05	0.00	0.01
Sum	100.00	100.00	100.00	100.00	100.00	100.00	100.00	100.00	100.00	100.00	100.00	100.00	100.00	100.00	100.00	100.00	100.00	100.00	100.00	100.00

[a]Fatty acid (FA) identities in the form of carbon number: degree of unsaturation, C:U.
[b]Isomers not differentiated by LC-MS, so not specified here. Complete FA composition including isomers reported separately.

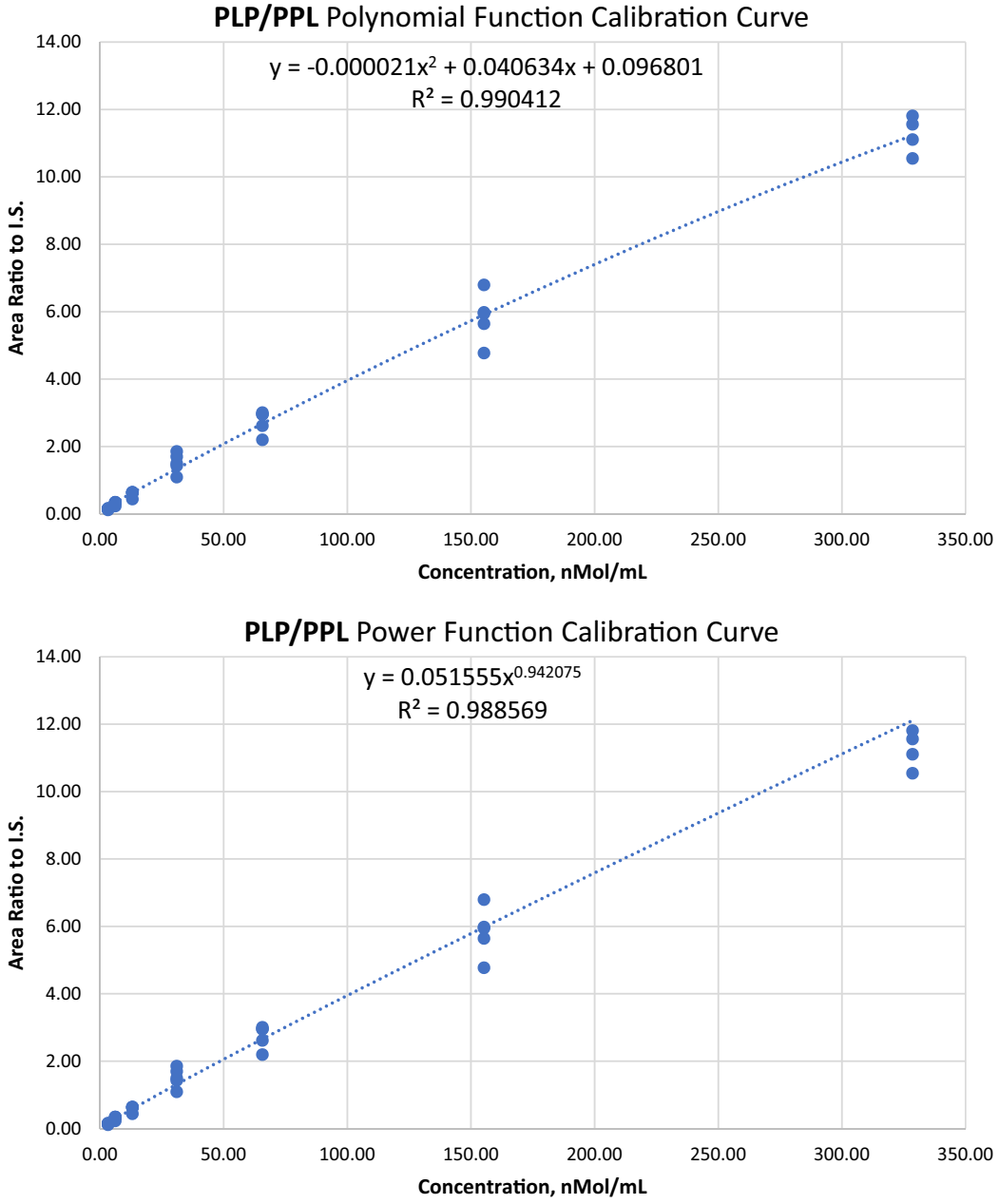

FIGURE 7 Calibration curves for PLP/PPL using (a) a polynomial function, and (b) a power function. The polynomial function gives less error at the high end of concentrations, while the power function gives less error at the lowest concentrations

TAG regioisomer calibration lines

As mentioned in the Materials section, calibration curves were made of two sets of regioisomer standards that were intertwined to produce a single set with alternating regioisomer quantities. Thus, in addition to the calibration curves such as shown in Figure 7, a second set of calibration lines for regioisomers was produced from the ratios of $[DAG]^+$ fragments in ESI-MS/MS spectra. For TAG standards, the beginning and ending retention times of peak integration were manually input into the Xcalibur Qual Browser, and the peak list was captured and pasted into a Microsoft Excel spreadsheet. $[DAG]^+$ peak areas for the $[AA]^+$ and $[AB]^+$ fragments from Type II TAGs (Byrdwell, 2005a, 2015b, 2016) (ABA/AAB/BAA) were used to calculate Critical Ratio 2 (Byrdwell, 2005a, 2015b, 2016), $[AA]^+/[AB]^+$. The $[AA]^+$ and $[AB]^+$ fragments from pulse TAGs identified by LipidSearch were obtained in a similar fashion by inputting the beginning and ending retention times from LipidSearch into the Xcalibur Qual Browser and then capturing the peak list for each integrated peak.

Table S3 lists the Critical Ratio 2 (CR2) values for TAG standards, taken from the calibration curves produced for each of the TAGs in the calibration mixture, while Figure S7 shows the plot of the

CR2 values in ascending order, allowing trends to be seen. Figure S7 shows that the range of CR2 values increased with increasing chain length. For instance, $CR2_{LPL/LLP} < CR2_{LOL/LLO}$ and $CR2_{OPO/OOP} < CR2_{OSO/OOS} < CR2_{OAO/OOA}$. And the degree of unsaturation also affected the CR2 values, such as $CR2_{OSO/OOS} < CR2_{OLO/OOL}$ and $CR2_{POP/PPO} < CR2_{PLP/PPL}$. The one TAG having the longest FA chains and the highest degree of unsaturation, ODhO/OODh, gave values out of the range of all other TAGs. The ranges in Table S3 and Figure S7 are a little higher with narrower ranges than the values obtained by Holčapek et al. (2010) on a ThermoScientific LTQ Orbitrap XL mass spectrometer, which were obtained using silver chromatography with a hexane/2-propanol/acetonitrile solvent system.

The amounts of regioisomer TAGs that were present in pulses and in the calibration mixture were determined using calibration lines made from the pure regioisomers in Table S3. The amounts of ABA (versus AAB and BAA) regioisomers of pulse TAGs are given in Table S4. LLO and LLP mostly had the two 'L' moieties together, instead of in the outer stereospecific numbering (*sn*)-1,3 positions. On the other hand, PLP and POP preferentially had 'P' in the *sn*-1,3 positions. These data indicate that the regioisomer compositions of TAGs can be readily determined, but it is better to have regioisomer standards run under the same conditions as samples than to rely on CR values from literature.

The overall positions of FAs in TAGs has been determined by Yoshida et al. using enzymatic hydrolysis in adzuki beans (*Vigna angularis*) (Yoshida et al., 2010), broad beans (*Vicia faba*) (Yoshida et al., 2009), jack beans (*Canavalia gladiata*) (Yoshida et al., 2013) and peas (*Pisum sativum*) (Yoshida et al., 2007b) but these analyses do not inform the identities of individual molecular species, only the overall trend.

Oxidation products

Several peaks appeared that had masses that were 16 amu larger than normal TAGs and gave fragments 16 amu larger than normal $[DAG]^+$ fragments. The HRAM masses indicated that these were oxo-TAGs. The addition of 16 amu indicated that the oxo-TAGs were likely either hydroxy TAGs ($-H + OH = \Delta 16$) or epoxy TAGs in which an oxygen attached to the two carbons of a double bond, without removing hydrogens ($+O = \Delta 16$). TAGs showing one oxo- or two oxo-groups are labeled in Figure 2, Figures S3, and Figure S4. The fatty acid methyl esters (FAME) of some oxo-FAs were qualitatively identified at low levels by GC–MS, showing addition of 16 amu, but were not quantified by GC-FID. Since oxo-TAGs were present at low levels, and no RFs were available for them, they were not quantified by LC–MS.

These oxidation products likely arose from long-term storage of the ground samples. Although the samples were nominally stored at −80°C, power outages and building power problems mean that they were likely subjected to higher temperatures on occasion, and the fact that they were already ground meant that a higher exposed surface area was present. Nevertheless, these samples were analyzed because data on their OS content had already been reported.

Tocopherol quantification

The short, fast chromatographic run did not allow tocopherols to be fully resolved, but instead they eluted as partially overlapped peaks at ∼1.16, 1.28, and 1.46 min for δ-, γ-, and α-tocopherols by APPI-MS, respectively. Tocopherols did not respond well to ESI without derivatization, and APPI-MS was not sensitive enough to quantify these at the levels present in pulses, but fluorescence detection allowed them to be quantified together as a group. The calibration standards included α-, β-, and γ-tocopherols at concentrations given in Table S1, and the calibration line of the total tocopherol concentration is given in Figure S8A. Since detection was by fluorescence, quantification was done using the external standard method. The least error in calculating concentrations of low level standards was obtained using response factors. A plot of the RFs versus concentration is given in Figure S8B. Since values in pulses (∼0.04 μg/ml) were just below the lowest calibration standard (∼0.05 μg/ml), the RF of the lowest standard was used. Nevertheless, the linearity of the calibration line ($R^2 = 0.9969$) indicated that combining the two sets of calibration standards into one intertwined set still produced FSV calibration lines with good linearity in the ng/ml to μg/ml range (0.05 μg/ml = 50 ng/ml).

The total amounts of tocopherols determined in the pulse extracts studied are given in Table S5. The tocopherol levels fell into a rather narrow range from 74 μg/100 g to 92 μg/100 g for these 10 extracts. The results obtained using the Folch extraction (1957) appear to much lower than values in the literature, which mostly used dedicated tocopherol analyses including a hexane or petroleum ether extraction. It appears that tocopherols were not quantitatively extracted using the chloroform/methanol extraction. Since tocopherols are present in substantial amounts in pulses, in the future it appears that we will need to use a more targeted neutral lipid extraction for those analytes.

Gopala Krishna et al. (1997) reported the tocopherols in petroleum ether extracts of Indian pulses, reporting total tocopherols of 6.76 mg/100 g for black gram pulses to 12.54 mg/100 g for green gram, being mostly (6.58 mg/100 g to 11.66 mg/100 g, respectively)

γ-tocopherol. These values were given in mg tocopherols per 100 g fat extracted, and were converted to mg/100 g sample using the fat % extracted. Other literature values were given units of mg/100 g sample. Padhi et al. (2017) reported tocopherol values from 2.253 mg/100 g (tocopherols summed and converted from μg/g) for hexane extracts of *cooked* cranberry beans (*Phaseolus vulgaris*) to 5.657 mg/100 g for cooked yellow whole peas (*Pisum sativum*), with γ-tocopherol from 2.253 mg/100 g to 5.417 mg/100 g, respectively. Cooked navy beans gave a value of 2.317 mg/100 g, all γ-tocopherol. Lentils ranged from 2.965 mg/100 g (red split lentils) to 4.618 mg/100 g (small green lentils).

CONCLUSION

This short, fast method was not expected to provide chromatographic resolution as good as that by longer separations. It was intended to be better than infusion, while still being high throughput. An intentional compromise was made between separation run length and TAG structural specificity provided. Nevertheless, by apportioning partially overlapped isomer fragment peaks, we were able to identify and semi-quantify many more TAG molecular species than expected from such a short separation. Peak shapes were surprisingly good. Even better resolution could likely be obtained using a sub-2 μm particle column, but those tend to clog more easily. For the sake of robustness of the method, a 2.6 μm particle column was employed.

Eliminating the need for subtracting model isotope contributions to overlapped TAGs, as required by infusion, made calculations simpler and eliminated the need for calculated theoretical isotope ratios.

Conversion of the percentage relative composition to absolute milligram quantities was not successful. Different responses of TAGs based on well documented effects of carbon chain length and degree of unsaturation caused the direct correlation between peak area and TAG amount to be lost after RFs were applied.

However, individual TAGs were quantified based on calibration standards. Obviously, this is not feasible for every TAG, due to limited availability and expense of pure TAG standards, therefore, an easy, ideal method for absolute TAG quantification by LC–MS remains elusive. For specific TAG regioisomer pairs we constructed regioisomer calibration lines from alternating concentration levels in the TAG quantification calibration curves. Two sets of mono-regioisomer (1,3- or 1,2-) TAG calibration standards were interweaved to give one set of standards with levels made of alternating regioisomers.

Two ranges of concentrations were used for different analytes: low-concentration linear ranges with high coefficients of determination, $r^2 > 0.99$, for FSVs (0.05–5.0 μg/ml), and non-linear power or polynomial calibration curves for the TAGs that are the bulk of the extract, present at 50- to 80-fold higher levels (~2.5–250 μg/ml, or ~4–411 nMol/ml). We hoped to quantify tocopherols directly from these extracts, but the extraction did not appear to quantitatively extract tocopherols. A dedicated extraction using highly nonpolar solvent appears necessary for accurate tocopherol quantification.

Despite the shortcomings of such a fast method, we were able to produce TAG mole percent relative compositions of pulses and use those to identify clusters of pulses grouped by similarity in their TAG compositions. We calculated the FA compositions from the TAG compositions and demonstrated that the FAs also gave the same clusters. We demonstrated a new approach to making calibration curves from mixed sets of regioisomers and used those to quantify the relative amounts of individual TAG molecular species regioisomers. These data provide valuable new information about the TAG compositions of pulses and trends within them.

AUTHOR CONTRIBUTIONS

William Craig Byrdwell conceived of the experiments, developed the LC–MS method, prepared calibration solutions, ran LC–MS instruments, manually integrated TAG and FSV peaks, and performed calculations. Hari Kiran Kotapati analyzed data using lipidomic software, manually confirmed peak identities, performed calculations, and produced tabulated areas. Robert Goldschmidt extracted samples, optimized the GC separations, performed quantitative GC-FID and qualitative GC–MS analyses, and produced tabulated areas.

ACKNOWLEDGMENTS

This work was supported by the USDA Agricultural Research Service. Mention or use of specific products or brands does not represent or imply endorsement by the USDA.

CONFLICT OF INTEREST

The authors declare that they have no conflicts of interest.

ETHICS STATEMENT

This article does not contain any studies with human subjects or animals.

ORCID

William Craig Byrdwell https://orcid.org/0000-0001-8241-428X

REFERENCES

Buchgraber M, Ulberth F, Emons H, Anklam E. Triacylglycerol profiling by using chromatographic techniques. Eur J Lipid Sci Technol. 2004;106:621–48. https://doi.org/10.1002/ejlt.200400986

Byrdwell WC. Dual parallel mass spectrometers for analysis of sphingolipid, glycerophospholipid and plasmalogen molecular

species. Rapid Commun Mass Spectrom. 1998;12:256–72. https://doi.org/10.1002/(SICI)1097-0231(19980314)12:5<256::AID-RCM149>3.0.CO;2-8

Byrdwell WC. The bottom-up solution to the triacylglycerol lipidome using atmospheric pressure chemical ionization mass spectrometry. Lipids. 2005a;40:383–417. https://doi.org/10.1007/s11745-006-1398-9

Byrdwell WC. Qualitative and quantitative analysis of Triacylglycerols by atmospheric pressure ionization (APCI and ESI) mass spectrometry techniques. In: Byrdwell WC, editor. Modern methods for lipid analysis by liquid chromatography/mass spectrometry and related techniques. Champaign, IL: AOCS Press; 2005b. p. 298–412.

Byrdwell WC. Quadruple parallel mass spectrometry for analysis of vitamin D and triacylglycerols in a dietary supplement. J Chromatogr A. 2013;1320:48–65. https://doi.org/10.1016/j.chroma.2013.10.031

Byrdwell WC. Critical ratios for structural analysis of triacylglycerols using mass spectrometry. Lipid Technol. 2015a;27:258–61. https://doi.org/10.1002/lite.201500054

Byrdwell WC. The updated bottom up solution applied to atmospheric pressure photoionization and electrospray ionization mass spectrometry. JAOCS, J Am Oil Chem Soc. 2015b;92:1533–47. https://doi.org/10.1007/s11746-015-2735-z

Byrdwell WC. The simulacrum system as a construct for mass spectrometry of triacylglycerols and others. Lipids. 2016;51:211–27. https://doi.org/10.1007/s11745-015-4101-1

Byrdwell WC. A note on the use of workstation software programs for quantification. J Liq Chromatogr Relat Technol. 2019;42:570–4. https://doi.org/10.1080/10826076.2019.1637350

Byrdwell WC. Analysis of lipids: Triacylglycerols, phospholipids, fatty acids and others. In: Shahidi F, editor. Bailey's industrial oil and fat products. 7th ed. Hoboken: John Wiley & Sons, Ltd; 2020. p. 293–336.

Byrdwell WC, Emken EA, Neff WE, Adlof RO. Quantitative analysis of triglycerides using atmospheric pressure chemical ionization-mass spectrometry. Lipids. 1996;31:919–35. https://doi.org/10.1007/BF02522685

Byrdwell WC, Kotapati HK, Goldschmidt R, Jakubec P, Nováková L. Three-dimensional liquid chromatography with parallel second dimensions, LC×2LC, and quadruple parallel mass spectrometry, LC3MS4, for infant formula analysis. J Chromatogr A. 2022;1661:462682.

Byrdwell WC, Neff WE, List GR. Triacylglycerol analysis of potential margarine base stocks by high-performance liquid chromatography with atmospheric pressure chemical ionization mass spectrometry and, flame ionization detection. J Agric Food Chem. 2001;49:446–57. https://doi.org/10.1021/jf0008801

Cao G, Ruan D, Chen Z, Hong Y, Cai Z. Recent developments and applications of mass spectrometry for the quality and safety assessment of cooking oil. TrAC—Trends Anal Chem. 2017;96:201–11. https://doi.org/10.1016/j.trac.2017.07.015

Dubois V, Breton S, Linder M, Fanni J, Parmentier M. Fatty acid profiles of 80 vegetable oils with regard to their nutritional potential. Eur J Lipid Sci Technol. 2007;109:710–32. https://doi.org/10.1002/ejlt.200700040

Duffin KL, Henion JD, Shieh JJ. Electrospray and tandem mass spectrometric characterization of acylglycerol mixtures that are dissolved in nonpolar solvents. Anal Chem. 1991;63:1781–8. https://doi.org/10.1021/ac00017a023

Dugo P, Kumm T, Cacciola F, Dugo G, Mondello L. Multidimensional liquid chromatographic separations applied to the analysis of food samples. J Liq Chromatogr Relat Technol. 2008;31:1758–807. https://doi.org/10.1080/10826070802128888

Dupont J, White PJ, Johnston KM, Alexander Heggtveit DH, McDonald BE, Grundy SM, et al. Food safety and health effects of canola oil. J Am Coll Nutr. 1989;8:360–75. https://doi.org/10.1080/07315724.1989.10720311

Fedeli E, Jacini G. Lipid composition of vegetable oils. Adv Lipid Res. 1971;9:335–82. https://doi.org/10.1016/b978-0-12-024909-1.50014-4

Ferreira H, Vasconcelos M, Gil AM, Pinto E. Benefits of pulse consumption on metabolism and health: a systematic review of randomized controlled trials. Crit Rev Food Sci Nutr. 2021;61:85–96. https://doi.org/10.1080/10408398.2020.1716680

Folch J, Lees M, Sloane-Stanley GH. A simple method for the isolation and purification of total lipides from animal tissue. J Biol Chem. 1957;226:497–509.

Gopala Krishna AG, Prabhakar JV, Aitzetmüller K. Tocopherol and fatty acid composition of some Indian pulses. JAOCS, J Am Oil Chem Soc. 1997;74:1603–6. https://doi.org/10.1007/s11746-997-0084-2

Gu Z-M, Ma J, Zhao X-G, Wu J, Zhang D. Reduction of nitriles to amines in positive ion electrospray ionization mass spectrometry. Rapid Commun Mass Spectrom. 2006;20:2969–72. https://doi.org/10.1002/rcm.2690

Hall C, Hillen C, Robinson JG. Composition, nutritional value, and health benefits of pulses. Cereal Chem. 2017;94:11–31. https://doi.org/10.1094/CCHEM-03-16-0069-FI

Han X, Gross RW. Quantitative analysis and molecular species fingerprinting of triacylglyceride molecular species directly from lipid extracts of biological samples by electrospray ionization tandem mass spectrometry. Anal Biochem. 2001;295:88–100. https://doi.org/10.1006/abio.2001.5178

Holčapek M, Dvorakova H, Lísa M, Giron AJ, Sandra P, Cvacka J. Regioisomeric analysis of triacylglycerols using silver-ion liquid chromatography-atmospheric pressure chemical ionization mass spectrometry: comparison of five different mass analyzers. J Chromatogr A. 2010;1217:8186–94. https://doi.org/10.1016/j.chroma.2010.10.064

Kotha RR, Finley JW, Luthria DL. Determination of soluble mono, Di, and oligosaccharide content in 23 dry beans (*Phaseolus vulgaris* L.). J Agric Food Chem. 2020;68:6412–9. https://doi.org/10.1021/acs.jafc.0c00713

Lavin M, Herendeen PS, Wojciechowski MF. Evolutionary rates analysis of leguminosae implicates a rapid diversification of lineages during the tertiary. Syst Biol. 2005;54:575–94. https://doi.org/10.1080/10635150590947131

Mahadevappa VG, Raina PL. Nature of some Indian legume lipids. J Agric Food Chem. 1978;26:1241–3. https://doi.org/10.1021/jf60219a044

Meiners CR, Derise NL, Lau HC, Ritchey SJ, Murphy EW. Proximate composition and yield of raw and cooked mature dry legumes. J Agric Food Chem. 1976;24:1122–6. https://doi.org/10.1021/jf60208a035

Mitchell DC, Marinangeli CPF, Pigat S, Bompola F, Campbell J, Pan Y, et al. Pulse intake improves nutrient density among us adult consumers. Nutrients. 2021;13:13. https://doi.org/10.3390/nu13082668

Omachi M, Homma S, Fujimaki M. Triacylglycerol composition of winged bean (*Psophocarpus tetragonolobus*). J Nutr Sci Vitaminol (Tokyo). 1987;33:49–54. https://doi.org/10.3177/jnsv.33.49

Padhi EMT, Liu R, Hernandez M, Tsao R, Ramdath DD. Total polyphenol content, carotenoid, tocopherol and fatty acid composition of commonly consumed Canadian pulses and their contribution to antioxidant activity. J Funct Foods. 2017;38:602–11. https://doi.org/10.1016/j.jff.2016.11.006

Podlaha O, Töregård B. A system for identification of triglycerides in reversed phase HPLC chromatograms based on equivalent carbon numbers. J High Resolut Chromatogr. 1982;5:553–8. https://doi.org/10.1002/jhrc.1240051007

Pryde EH. Composition of soybean oil. In: Erickson DR, Pryde EH, Brekke OL, Mounts TL, Falb RA, editors. Handbook of soy oil processing and utilization. Champaign, IL: American Oil Chemists' Society; 1980. p. 13–31.

Serrano C, Carbas B, Castanho A, Soares A, Patto MCV, Brites C. Characterisation of nutritional quality traits of a chickpea (*Cicer arietinum*) germplasm collection exploited in chickpea breeding in Europe. Crop Pasture Sci. 2017;68:1031–40. https://doi.org/10.1071/CP17129

U.S. Department of Agriculture ERS. Americans consumed almost 12 pounds of legumes per person in 2017. 2017. https://www.ers.usda.gov/data-products/chart-gallery/gallery/chart-detail/?chartId=92977#:~:text=U.S. Consumption of legumes reached, pounds per person in 2014 (accessed June 15, 2022).

United Nations Food and Agriculture Organization. Definition and classification of commodities: pulses and derived products. Pulses Deriv Prod 2022. http://www.fao.org/faoterm/viewEntry/en/?entryId=70035 (accessed September 20, 2022).

Xu S-L, Wei F, Xie Y, Lv X, Dong X-Y, Chen H. Research advances based on mass spectrometry for profiling of triacylglycerols in oils and fats and their applications. Electrophoresis. 2018;39:1558–68. https://doi.org/10.1002/elps.201700481

Xu T, Hu C, Xuan Q, Xu G. Recent advances in analytical strategies for mass spectrometry-based lipidomics. Anal Chim Acta. 2020;1137:156–69. https://doi.org/10.1016/j.aca.2020.09.060

Yoshida H, Tomiyama Y, Kita S, Mizushina Y. Lipid classes, fatty acid composition and triacylglycerol molecular species of kidney beans (Phaseolus vulgaris L.). Eur J Lipid Sci Technol. 2005;107:307–15. https://doi.org/10.1002/ejlt.200401078

Yoshida H, Tomiyama Y, Tanaka M, Mizushina Y. Characteristic profiles of lipid classes, fatty acids and triacylglycerol molecular species of peas (*Pisum sativum* L.). Eur J Lipid Sci Technol. 2007a;109:600–7. https://doi.org/10.1002/ejlt.200600219

Yoshida H, Tomiyama Y, Tanaka M, Mizushina Y. Distribution of fatty acids in triacylglycerols and phospholipids from peas (*Pisum sativum* L.). J Sci Food Agric. 2007b;87:2709–14. https://doi.org/10.1002/jsfa.3035

Yoshida H, Tomiyama Y, Yoshida N, Mizushina Y. Regiospecific distribution of fatty acids in triacylglycerols and phospholipids from broad beans (*Vicia faba*). Eur J Lipid Sci Technol. 2009;111:386–91. https://doi.org/10.1002/ejlt.200800036

Yoshida H, Tomiyama Y, Yoshida N, Saiki M, Mizushina Y. Lipid classes, fatty acid distributions and triacylglycerol molecular species of broad beans (*Vicia faba*). JAOCS, J Am Oil Chem Soc. 2008;85:535–41. https://doi.org/10.1007/s11746-008-1221-2

Yoshida H, Tomiyama Y, Yoshida N, Shibata K, Mizushina Y. Regiospecific profiles of fatty acids in triacylglycerols and phospholipids from adzuki beans (*Vigna angularis*). Nutrients. 2010;2:49–59. https://doi.org/10.3390/nu2010049

Yoshida H, Yoshida N, Kuriyama I, Tomiyama-Sakamoto Y, Mizushina Y. Profiles of lipid components, fatty acid distributions of triacylglycerols and phospholipids in Jack beans (*Canavalia gladiata* DC). Food Chem. 2013;136:807–12. https://doi.org/10.1016/j.foodchem.2012.08.087

Zeitoun MAM, Neff WE, Selke E, Mounts TL. Analyses of vegetable oil triglyceride molecular species by reversed phase high performance liquid chromatography. J Liq Chromatogr. 1991;14:2685–98. https://doi.org/10.1080/01483919108049348

SUPPORTING INFORMATION

Additional supporting information can be found online in the Supporting Information section at the end of this article.

How to cite this article: Byrdwell WC, Kotapati HK, Goldschmidt R. Fast chromatography of pulse triacylglycerols. J Am Oil Chem Soc. 2023;100(1):25–43. https://doi.org/10.1002/aocs.12665